

Stopping Dark Mesons in Their Tracks with Long-Lived Particle and Resonant Signatures

**Pouya Asadi,^a Austin Batz,^a Elias Bernreuther,^b Marco Costa,^c
Samuel Homiller,^d and Graham D. Kribs^a**

^a*Institute for Fundamental Science and Department of Physics,
University of Oregon, Eugene, OR 97403, USA*

^b*Department of Physics, University of California, San Diego, La Jolla, CA 92093, USA*

^c*Perimeter Institute for Theoretical Physics, 31 Caroline St N, Waterloo, ON N2L 2Y5, Canada*

^d*Laboratory for Elementary Particle Physics, Cornell University, Ithaca, NY 14853, USA*

E-mail: pasadi@uoregon.edu, abatz@uoregon.edu, ebereuther@ucsd.edu,
mcosta1@perimeterinstitute.ca, shomiller@cornell.edu, kribs@uoregon.edu

ABSTRACT: Dark sectors with confining gauge interactions can provide both simple dark matter candidates and striking signals at colliders. We recast Large Hadron Collider searches for two different signatures of dark mesons that arise from a strongly-coupled theory with vector-like dark quarks that are in some non-trivial representation of Standard Model $SU(2)_L$. For any such electroweak representation, there is a 3-plet of dark mesons whose charged components are long-lived, and we reinterpret searches for disappearing tracks to place a lower bound on their mass of ~ 1.2 TeV. When the dark quarks are in $SU(2)_L$ representations larger than the fundamental, there is also a 5-plet of dark mesons that interacts with the electroweak gauge bosons via a chiral anomaly. We show that the 5-plet is the unique non-trivial meson multiplet with this anomaly and recast searches for the resulting diboson resonances to place bounds on model parameters. With additional measurements, the anomaly also enables one to reconstruct some ultraviolet parameters (the numbers of dark flavors and colors) while only measuring states in the infrared. Each of these signals represents an exciting opportunity for future searches using higher luminosity.

Contents

1	Introduction	1
2	The Model	3
2.1	Mesons in the Chiral Effective Theory	4
2.2	Dark G -Parity	5
2.3	Meson Masses	7
3	The 5-plet Anomaly	10
3.1	Review of Standard Model Meson Anomalies	10
3.2	Uniqueness of the 5-plet Anomaly	11
4	Collider Signals and Constraints	15
4.1	Disappearing Tracks: A 3-plet Signature	15
4.2	Anomaly-induced Resonances: A 5-plet Signature	18
5	Conclusion	22
A	Obtaining Flavor Generators	25
B	Computing the 5-plet Anomaly	26

1 Introduction

While new physics is required to explain dark matter, the Standard Model (SM) has maintained remarkable consistency with various kinds of experiments over many years. Many searches for new physics have focused on minimal extensions of the SM and have placed stringent bounds on them. This motivates exploring directions beyond the most minimal models. At the same time, simple models with concrete predictions serve as useful benchmarks to target in experimental searches. Confining dark sectors can simultaneously provide this non-minimality and simplicity. In such models, the SM is extended by a non-abelian gauge interaction with dark quarks in the ultraviolet (UV) that bind into dark hadrons in the infrared (IR). The UV theory may contain only a few degrees of freedom while the IR theory consists of a rich spectrum of states with a variety of possible interactions with the SM.

New confining sectors have motivated numerous dedicated searches at the Large Hadron Collider (LHC) [1–10], as well as reinterpretations of other searches [11–15]. Depending on the dark quark masses, confinement scale, number of flavors,

number of colors, and the portal to the SM, these models can give rise to various intriguing signatures. Examples include long-lived particles [16–24], novel shower patterns [25–38], and exotic phenomena such as quirks [39–41]. See Refs. [42] and [43] for reviews. Of particular importance to this work is the variety of potential dark hadron production mechanisms. New particles with electroweak interactions can of course be pair-produced at sufficiently high energies via Drell-Yan (DY) and vector boson fusion (VBF), but other possibilities including vector mesons mixing with gauge bosons [12, 16] and single production of pion-like states through chiral anomalies [28] exist as well. As we will show, correlations between the rates of these processes can even shed light on details of the UV theory.

We study collider signals of models with a confining dark sector that include vector-like dark quarks in the N_f -dimensional representation of SM $SU(2)_L$, in addition to being charged under the new $SU(N_c)$. See Refs. [11, 12, 16, 31, 44–48] for similar models. It was recently discovered [49] that this model has a natural \mathbb{Z}_2 symmetry, known as \mathcal{H} -parity, that forbids the leading electromagnetic moments of the neutral dark hadrons. This observation on its own significantly relaxes naïvely stringent direct detection constraints on the dark baryons as dark matter candidates. It was additionally pointed out in Ref. [50] that the lightest dark baryons are pure or approximate SM singlets for many combinations of N_c and N_f , which even further suppresses direct detection signals of these so-called Noble Dark Matter candidates. The counter-intuitive implication is that while the dark quarks are electrically charged, the dark sector may be more readily discovered at colliders than other types of experiment. This is the possibility we investigate in this paper. Even beyond the underlying dark matter motivations, we will explore various interesting features of collider phenomenology that arise in the presence of heavy dark hadrons whose constituents are in an arbitrary $SU(2)_L$ representation.

We consider the regime where the mass of the dark quarks is significantly *below* the dark sector confinement scale. This allows us to exploit our knowledge of SM quantum chromodynamics (QCD) and work in an effective field theory (EFT) of dark mesons. We focus on the limit where the pseudo-Nambu–Goldstone bosons (pNGBs) of chiral symmetry breaking in the dark sector are the only dark hadrons that are kinematically accessible in experiments at the LHC.

We analyze two under-explored signals of these confining dark sectors. The first is disappearing tracks from long-lived dark mesons, and the second is resonant diboson production from singly produced dark meson decays. These signatures allow us to reinterpret existing LHC searches to constrain our model parameters. Moreover, the model is an excellent benchmark for future searches targeting the same final states.

For all $N_f \geq 2$, there is an $SU(2)_L$ 3-plet of pNGBs denoted by $\hat{\pi}_3$. For dark hadron mass scales within the regime we consider (*i.e.* above the scale of electroweak symmetry breaking), there is a ~ 170 MeV mass splitting between the charged and neutral components of the $\hat{\pi}_3$ [51]. These mesons are forbidden from decaying directly

to the SM by a \mathbb{Z}_2 known as G -parity (which is related to \mathcal{H} -parity and an analogous \mathbb{Z}_2 in the SM, as explained in Sec. 2.2) [44]. The dark G -parity has such importance that we denote G -odd pNGBs by $\hat{\pi}$ and G -even pNGBs by $\hat{\eta}$, loosely following an analogy to SM mesons. The charged components of the $\hat{\pi}_3$ (denoted $\hat{\pi}_3^\pm$) decay to the neutral component $\hat{\pi}_3^0$ by emitting an SM pion, and the small phase space for this process causes the $\hat{\pi}_3^\pm$ to be long-lived. The $\hat{\pi}_3^\pm$ are therefore targets for long-lived particle (LLP) searches with signals very similar to those of charginos [52, 53]. When the charged meson decays inside a detector’s inner tracker and the soft pion is not reconstructed, this leaves a signature known as a disappearing track. In Sec. 4.1, we use disappearing track searches to derive a lower bound on this meson’s mass.

We also study the single production of specific meson species. If $N_f \geq 3$, there is an $SU(2)_L$ 5-plet of pNGBs (denoted by $\hat{\eta}_5$) in the spectrum that is *unique* in that it is the only representation of dark mesons that has an anomaly with $SU(2)_L$. As explained in Sec. 3, this is analogous to the SM neutral pion’s anomaly with quantum electrodynamics (QED). This anomaly allows the $\hat{\eta}_5$ to be resonantly produced via VBF before decaying to a pair of electroweak bosons. The rate for this process depends on N_f and f_π/N_c , where f_π is the dark pion decay constant. Thus, measuring these anomaly-induced collider signals would reveal details of the UV model. Similar examples of bound state resonances have been considered in Refs. [54–57]. We use searches for scalar resonances decaying to diboson final states to place constraints on f_π/N_c in Sec. 4.2.

2 The Model

We study dark mesons arising from a new strongly-coupled confining gauge sector with the Lagrangian

$$\mathcal{L}_{\text{dark}} = -\frac{1}{4}G^{\mu\nu a}G_{\mu\nu}^a + \bar{\mathbf{Q}}(i\not{D} - m_0)\mathbf{Q}, \quad (2.1)$$

where $G_{\mu\nu}^a$ is the field strength of the dark $SU(N_c)$, and \mathbf{Q} is a vector-like dark quark with mass m_0 that transforms as a fundamental of $SU(N_c)$ and an N_f -plet of $SU(2)_L$ with $N_f \geq 2$. Since the quarks transform in the N_f -dimensional representation of $SU(2)_L$, one can think of $SU(2)_L$ as a gauged subgroup of an $SU(N_f)$ flavor symmetry. Gauge invariance requires the flavor multiplet to have degenerate mass at tree level. The quarks have vanishing hypercharge, so each dark sector particle has an electric charge equal to its weak isospin. At low energies, these quarks bind into dark mesons and baryons.

As pointed out in Ref. [49], this model has a \mathbb{Z}_2 symmetry known as \mathcal{H} -parity, under which the fields transform as

$$\mathbf{Q} \xrightarrow{\mathcal{H}} e^{i\pi J_y} \mathbf{Q}, \quad W_\mu^i \xrightarrow{\mathcal{H}} \mathcal{C} W_\mu^i \mathcal{C}, \quad B_\mu \xrightarrow{\mathcal{H}} \mathcal{C} B_\mu \mathcal{C}, \quad (2.2)$$

where J_y is the second generator of $SU(2)_L$, W_μ^i is the mediator of $SU(2)_L$, B_μ is the mediator of $U(1)_Y$, and \mathcal{C} denotes charge conjugation. The neutral dark quarks and hadrons in odd representations of $SU(2)_L$ are eigenstates of \mathcal{H} with eigenvalue ± 1 , whereas \mathcal{H} maps charged states to opposite-charge states (up to a sign). \mathcal{H} -parity has great importance for the dark matter phenomenology of the dark baryons, as explored in Refs. [49, 50].

While mesons also transform under \mathcal{H} -parity, there is a slightly different \mathbb{Z}_2 known as G -parity [44] that has direct implications for meson phenomenology. As we explain in Sec. 2.2, G -parity selection rules imply large hierarchies between the meson lifetimes.

2.1 Mesons in the Chiral Effective Theory

This work focuses on the light quark limit, where the dark quark mass is significantly smaller than the dark sector confinement scale. In this limit, we can use an effective theory of dark mesons — the chiral Lagrangian — and trade the UV parameters of the quark mass and confinement scale for the IR parameters of the lightest dark meson mass m_π and the dark pion decay constant f_π .

Since our regime is similar to that of the light mesons in QCD, we can borrow much intuition from the SM. The $U(N_f)_L \times U(N_f)_R$ flavor symmetry in the massless limit of Eq. (2.1) is spontaneously broken during confinement by the quark condensate $\langle \bar{\mathbf{Q}} \mathbf{Q} \rangle$ to its diagonal $SU(N_f)$ subgroup, plus a $U(1)$ associated with a dark baryon number. There are $N_f^2 - 1$ light pseudo-scalar pNGBs in addition to a heavy flavor-singlet $\hat{\eta}'$ that is the would-be pNGB of the anomalous axial $U(1)$. Explicit breaking of $U(N_f)_L \times U(N_f)_R$ by the quark masses and gauging its $SU(2)_L$ subgroup gives mass to the pNGBs, as further explained in Sec. 2.3.

Each meson species transforms in some representation of $SU(2)_L$ that determines its interactions with the SM. A meson flavor state is a superposition of states with a quark flavor and an anti-quark flavor. Both the quark and the anti-quark are in the self-conjugate representation \mathbf{N}_f of $SU(2)_L$, so the mesons are organized into the irreducible representations in

$$\mathbf{N}_f \otimes \mathbf{N}_f = \bigoplus_{m=1}^{N_f} (\mathbf{2m} - \mathbf{1}) = \mathbf{1} \oplus \mathbf{3} \oplus \mathbf{5} \oplus \cdots \oplus (\mathbf{2N}_f - \mathbf{1}). \quad (2.3)$$

For the lowest-lying pseudo-scalar mesons, we can identify the $\mathbf{3}, \mathbf{5}$, *etc.* as the representations of the pNGBs and the flavor-singlet $\mathbf{1}$ as the would-be pNGB $\hat{\eta}'$. Note in particular that there is always a 3-plet $\hat{\pi}_3$ (since $N_f \geq 2$), and there is a 5-plet $\hat{\eta}'_5$

for all $N_f \geq 3$. In the rest of this work, we explore the interesting features that arise for each of these meson representations and the consequences for phenomenology.

2.2 Dark G -Parity

This model has a \mathbb{Z}_2 symmetry known as G -parity [44] that has important implications for the dark mesons and has an analogy in the SM [58, 59]. Let us first review the SM case. The isospin group $SU(2)_I$, which acts on u and d quarks, is a subgroup of the $SU(3)$ flavor symmetry that acts on u , d , and s quarks.¹ Besides the would-be pNGB SM η' , there is an $SU(3)$ octet of pNGBs containing an iso-triplet (the pions), two iso-doublets (the kaons), and an iso-singlet (the SM η).² The SM G -parity transformation is $G_{\text{SM}} = \mathcal{C}e^{i\pi I_y}$ (where I_y is the second generator of $SU(2)_I$), which has eigenstates

$$\eta'_{\text{SM}} \xrightarrow{G_{\text{SM}}} \eta'_{\text{SM}}, \quad \pi_{\text{SM}} \xrightarrow{G_{\text{SM}}} -\pi_{\text{SM}}, \quad \eta_{\text{SM}} \xrightarrow{G_{\text{SM}}} \eta_{\text{SM}}, \quad (2.4)$$

among the lowest-lying pseudo-scalar mesons. The G_{SM} charge of a more general meson is $(-1)^{I+\ell+s}$, where $I \in \{0, 1\}$ is the isospin, ℓ is the orbital angular momentum of the constituent quarks, and s is the total spin of the constituent quarks [59]. SM G -parity is preserved by QCD, which leads to selection rules such as the forbidding of the $\eta_{\text{SM}} \rightarrow 3\pi_{\text{SM}}^0$ decay as a strong process [60]. However, SM G -parity is violated at tree-level by QED. After all, $\eta_{\text{SM}} \rightarrow 3\pi_{\text{SM}}^0$ is one of the principal decay modes of the η_{SM} . By contrast, G -parity in the dark sector provides much stronger selection rules.

The dark G -parity transformation on dark sector matter content is [44]

$$G = \mathcal{C}e^{i\pi J_y} = \mathcal{C}\mathcal{H}, \quad (2.5)$$

where the isospin rotation in the SM G -parity definition has been replaced by a global $SU(2)_L$ rotation.³ Clearly, G and \mathcal{H} are closely related. A key difference is that G maps particles to anti-particles, while \mathcal{H} maps a particle to a different particle in the same electroweak multiplet, up to a sign. In the case of baryons, G maps a baryon to an anti-baryon, so a baryon cannot be G eigenstate even if it can be an \mathcal{H} eigenstate. Mesons, however, have particles and anti-particles *in the same electroweak multiplet*, so they can be eigenstates of G , \mathcal{H} , or both.

¹ $SU(2)_I$ is embedded in flavor $SU(3)$ in the SM differently from how $SU(2)_L$ is embedded in $SU(N_f)$ in the dark sector. In our model, the fundamental of $SU(N_f)$ is identified with the \mathbf{N}_f of $SU(2)_L$, while the fundamental of flavor $SU(3)$ in the SM is identified with $\mathbf{1} \oplus \mathbf{2}$ of $SU(2)_I$.

²More precisely, the SM η and η' mass eigenstates are admixtures of the flavor singlet and flavor octet. We comment on mass mixings of dark sector flavor states in Sec. 2.3.

³ G also acts as charge conjugation on the dark gluon field so that the dark $SU(N_c)$ coupling is G -even [44].

Consider a meson state $|J, Q\rangle$ in the $2J+1$ -dimensional representation of $SU(2)_L$ with electric charge Q . That is,

$$J_z|J, Q\rangle = Q|J, Q\rangle, \quad (2.6)$$

$$J^2|J, Q\rangle = J(J+1)|J, Q\rangle, \quad (2.7)$$

where J_z is the third generator of $SU(2)_L$, and J^2 is the quadratic Casimir operator. Following the SM analogy, the actions of the various \mathbb{Z}_2 transformations can be self-consistently written as

$$\mathcal{H}|J, Q\rangle = (-1)^{J-Q}|J, -Q\rangle, \quad (2.8)$$

$$\mathcal{C}|J, Q\rangle = (-1)^{Q+s+\ell}|J, -Q\rangle, \quad (2.9)$$

$$G|J, Q\rangle = (-1)^{J+s+\ell}|J, Q\rangle. \quad (2.10)$$

One can see from these transformation rules that *every meson state in a particular electroweak multiplet is an eigenstate of G -parity*. We focus on the pseudo-scalar pNGBs in this work, so we set $s = \ell = 0$ from now on.

Recall from Eq. (2.3) that the mesons appear in the $\mathbf{1}, \mathbf{3}, \mathbf{5}, \dots$ representations of $SU(2)_L$. Therefore, Eq. (2.10) implies that the meson multiplets have alternating G -parity, *i.e.* the singlet, 5-plet, 9-plet, *etc.* are G -even, and the 3-plet, 7-plet, 11-plet, *etc.* are G -odd. To make our meson naming scheme explicit, we denote the G -odd pNGBs as $\hat{\pi}$ and the G -even pNGBs as $\hat{\eta}$. We also specify the $SU(2)_L$ representations of each meson with subscripts and electric charges with superscripts when necessary. Again, we emphasize that only the neutral components of electroweak multiplets have well-defined \mathcal{H} -parity, while entire meson multiplets have well-defined G -parity.

Dark G -parity can be broken by the dimension-5 effective operators [44]

$$B_{\mu\nu}\overline{\mathbf{Q}}\sigma^{\mu\nu}\mathbf{Q} \xrightarrow{G} B_{\mu\nu}(\mathcal{C}\overline{\mathbf{Q}}\sigma^{\mu\nu}\mathbf{Q}\mathcal{C}) = -B_{\mu\nu}\overline{\mathbf{Q}}\sigma^{\mu\nu}\mathbf{Q}, \quad (2.11)$$

$$H^\dagger\tau^a H\overline{\mathbf{Q}}J^a\mathbf{Q} \xrightarrow{G} H^\dagger\tau^a H\overline{\mathbf{Q}}(e^{-i\pi J_y}J^ae^{i\pi J_y})\mathbf{Q} = H^\dagger\tau^a H\overline{\mathbf{Q}}(-J^a)^*\mathbf{Q}, \quad (2.12)$$

where $B_{\mu\nu}$ is the hypercharge field strength, H is the Higgs doublet, and τ^a is a generator of the fundamental representation of $SU(2)_L$. However, unlike SM G -parity, there are no gauge-invariant renormalizable operators that violate the dark G -parity.⁴ This quasi-stabilizes the lightest G -odd meson, which is the $\hat{\pi}_3^0$. As noted in Refs. [44, 49], if these operators are suppressed by the Planck scale, then the quasi-stable $\hat{\pi}$ mesons produced in the early universe may survive past Big Bang Nucleosynthesis but be too short-lived to be cosmologically safe. By dimensional analysis, we can roughly estimate the scaling of the $\hat{\pi}_3^0$ lifetime τ_3 with the scale of

⁴ \mathcal{H} -parity is violated at two-loop order by the SM due to its action on the hypercharge field [49]. By contrast, G leaves all SM fields invariant.

G -parity breaking $\Lambda_{\mathcal{G}}$ as

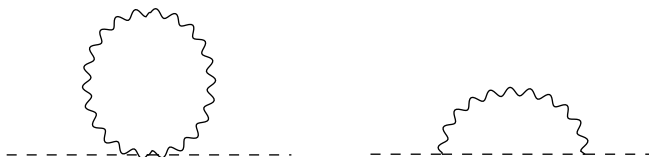
$$\tau_3 \sim \frac{a^2 \Lambda_{\mathcal{G}}^2}{m_\pi^3}, \quad (2.13)$$

$$\Lambda_{\mathcal{G}} \sim \frac{10^{16} \text{ GeV}}{a} \sqrt{\left(\frac{m_\pi}{1 \text{ TeV}}\right)^3 \left(\frac{\tau_3}{0.1 \text{ s}}\right)}, \quad (2.14)$$

where $a > 1$ is a dimensionless coefficient encapsulating coupling and phase space factors. To ensure $\tau_3 \lesssim 0.1 \text{ s}$ (so that the decays do not disrupt nucleosynthesis [61, 62]), $\Lambda_{\mathcal{G}}$ should be below $\sim 10^{16} \text{ GeV}$ when $m_\pi \sim \mathcal{O}(1) \text{ TeV}$. Therefore, we need some UV completion below the Planck scale to facilitate these decays. It was also noted in Ref. [50] that a UV completion below the Planck scale is required for many values of N_c and N_f to address sub-Planckian Landau poles of the electroweak coupling, and such a UV completion could also provide the needed G violation. While these G -parity violating decays may themselves have interesting phenomenology and help probe the scale of the UV completion, we do not consider them in this work. The lifetime could easily be well beyond the detector scale, and so we treat the $\hat{\pi}_3^0$ as stable in our collider study in Sec. 4.

2.3 Meson Masses

The chiral effective theory we employ has a regime of validity up to a UV mass scale of $\sim 4\pi f_\pi$. We therefore restrict our discussion to the range of pNGB masses below that scale, but there is some subtlety in the mass spectrum of the different pseudo-scalar species. The pNGBs get their masses from explicit breaking of chiral symmetry, of which there are two sources: quark masses and the gauging of the $SU(2)_L$ subgroup. The quark masses are degenerate at tree-level, so the pNGB masses are as well. Mass splittings arise due to loops with electroweak bosons of the form



that depend on the meson charge and representation. First, consider the mass splitting between mesons in different electroweak multiplets. The diagram on the left is quadratically divergent, so a meson in the $2J + 1$ -dimensional representation of $SU(2)_L$ gets a dominant correction to its mass-squared of $\sim 4\pi\alpha_W J(J + 1)f_\pi^2$, where α_W is the $SU(2)_L$ coupling [44]. Even in the massless quark limit, this prevents m_π from being much smaller than f_π without fine-tuning. Then, the difference in the squared masses of the pNGB multiplets scales like the difference in their quadratic Casimirs, but we cannot precisely compute it in perturbation theory.

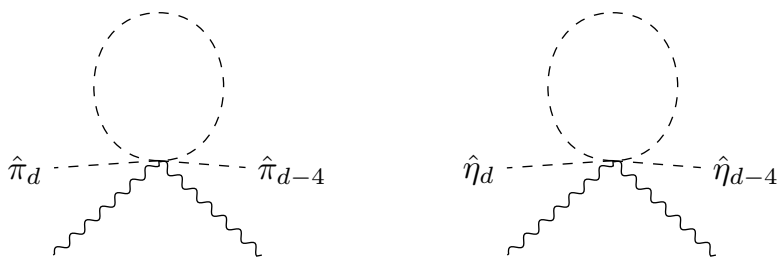
Next, consider the mass splitting between mesons with different charges in the same electroweak multiplet. The same kinds of loops contribute, but the splitting is due to electroweak symmetry breaking rather than the cutoff of the EFT. The calculation is performed in Ref. [51], and the splitting is ~ 170 MeV between singly-charged and neutral components of a multiplet for meson masses above $\mathcal{O}(100)$ GeV.

The splittings between components of the electroweak multiplets have a strong impact on the $\hat{\pi}$ meson lifetimes, as they are forbidden from decaying directly to the SM by G -parity. Therefore, charged $\hat{\pi}$ mesons decay via cascade, *i.e.* they decay to a lighter species in the same electroweak multiplet by radiating one or two off-shell gauge bosons, and the lighter species (if charged) then decays in the same way. This implies the singly-charged $\hat{\pi}$ mesons can decay as $\hat{\pi}^\pm \rightarrow \hat{\pi}^0 \pi_{\text{SM}}^\pm$, as the far off-shell W^\pm radiated by the $\hat{\pi}^\pm$ effectively mixes with the SM pion. There is additional discussion of this process in Refs. [63, 64], and the resulting decay rate is⁵

$$\Gamma(\hat{\pi}^\pm \rightarrow \hat{\pi}^0 \pi_{\text{SM}}^\pm) = \pi \alpha_W^2 \frac{f_{\pi, \text{SM}}^2}{m_W^4} J(J+1) \Delta m_{+,0}^2 \sqrt{\Delta m_{+,0}^2 - m_{\pi, \text{SM}}^2}, \quad (2.15)$$

where $f_{\pi, \text{SM}} \simeq 92$ MeV is the SM pion decay constant, J indicates the $\hat{\pi}$ meson representation, m_W is the W boson mass, $\Delta m_{+,0}$ is the splitting between the singly-charged and neutral $\hat{\pi}$ mesons, and $m_{\pi, \text{SM}}$ is the SM pion mass.⁶ The small phase space for this decay causes the $\hat{\pi}_3^+$ to be long-lived on a collider scale with proper lifetime τ roughly between 4 cm and 6 cm (depending on the mass). We explore the consequences for phenomenology in Sec. 4.1.

The mass splittings between different multiplets implies that the higher multiplets can decay by “hopping” down to a lower one. These processes are permitted by loop diagrams of the form [44]



with some dark meson species in the loop. These six-point vertices arise from dimension-6 effective operators in the meson EFT. In this way, mesons in repre-

⁵As discussed in Ref. [63], decays with leptonic final states are suppressed to the extent that the charged state would be collider-stable if the hadronic channel were not open. This is in part due to multi-body phase space suppression.

⁶One can compute the corresponding rate for a higher-charge $\hat{\pi}$ meson to decay to $\hat{\pi}$ meson with one less charge by replacing $J(J+1)$ in Eq. (2.15) with the square of the corresponding element of the $\text{SU}(2)_L$ ladder operator in the appropriate representation.

representations larger than the **5** can hop down to a meson in a lower representation with the same G -parity by emitting two electroweak bosons. Since these decays are facilitated by dimension-6 operators, we expect the decay rate to scale with the model parameters as

$$\Gamma_{\text{hop}} \sim \alpha_W^2 \frac{\Delta m_{d,d-4}^5}{(4\pi)^5 f_\pi^4}, \quad (2.16)$$

where $\Delta m_{d,d-4}$ is the splitting between the initial and final meson multiplets. While this decay rate is suppressed by a loop factor and multi-body phase space, the mass splitting itself is expected to scale as f_π . Moreover, the divergence of the loop introduces an additional numerical enhancement. Therefore, we expect the higher multiplets to rapidly decay to the $\hat{\pi}_3$ or $\hat{\eta}_5$ in this way.

This work focuses on the limit where the pNGBs are light enough to be accessible at the LHC while the heavier mesons (the $\hat{\eta}'$, vector mesons $\hat{\rho}$, *etc.*) are inaccessible. The reason is to avoid various complications such as the $\hat{\rho}$ mixing with the SM Z boson [12], interactions of the pNGBs with the $\hat{\rho}$, and the tower of other excited meson states. Indeed, many excited QCD resonances appear within an $\mathcal{O}(1)$ factor of the SM ρ mass [59], so we expect the same to be true in the dark sector. We generically expect these heavier meson masses to be $\sim 4\pi f_\pi$, so we will take $4\pi f_\pi$ to be above some threshold (below which some resonance searches may be sensitive) to safely ignore them. One possible exception, depending on the details of the UV, is the $\hat{\eta}'$, which becomes light in the large- N_c limit [65]. A light $\hat{\eta}'$ would slightly alter phenomenology for reasons that will become clear in Sec. 3, but we neglect this possibility in the rest of this work.

To get a rough estimate of the minimum mass where the $\hat{\rho}$ may be visible, we can compare our model to the similar dark sector described in Refs. [47] and [12] with dark vector mesons mixing with SM gauge bosons. There are dilepton resonance searches [66, 67], as well as the search in Ref. [4] for the vector meson in the similar model decaying to pairs of pNGB mesons. These searches probe the vector mass scale up to ~ 2 TeV at most, so this serves as a rough lower bound on $4\pi f_\pi$ above which the signals discussed in this work are dominant.

Another possible complication is mixing of mesons in different electroweak multiplets. This is in some sense analogous to SM η - η' mixing, but it is clearly only permitted in the dark sector by electroweak symmetry breaking. Ref. [50] shows how mixing of baryon multiplets is important to understanding their dark matter phenomenology, but the effect disappears as the relevant mass scales in the dark sector become larger than the electroweak scale. Also, if any of the dark sector mass scales were below the electroweak scale, then the details of the electroweak interactions between individual quarks may significantly alter the meson spectrum, as was the case for baryons in Ref. [50]. We neglect these effects in this work, as the relevant scales are set by $4\pi f_\pi$.

In summary, the mass splitting between the multiplets is set by the Casimirs and f_π , the splitting between entries within a multiplet is small and leads to long-lived $\hat{\pi}_3^\pm$ states, and the pNGBs are the only mesons we consider in our collider study. We have yet to discuss the decays of the $\hat{\eta}_5$ mesons, for which we need the findings of Sec. 3. This will show that each meson multiplet has its own idiosyncrasies with direct impact on experimental signals.

3 The 5-plet Anomaly

This section presents the striking result that not only can the $\hat{\eta}_5$ be singly produced and decay via an anomaly with $SU(2)_L$, but also that it is *unique* among the pNGBs in this way. The gauge-invariant form of the Wess-Zumino-Witten [68–70] operator contains the dimension-5 effective operator [44, 71, 72]

$$\mathcal{L}_{\text{anomaly}} = \frac{g_W^2}{16\pi^2} \frac{N_c}{f_\pi} \hat{\phi}^a \varepsilon^{\mu\nu\alpha\beta} W_{\mu\nu}^i W_{\alpha\beta}^j \text{Tr} [T^a J^i J^j], \quad (3.1)$$

where $g_W = \sqrt{4\pi\alpha_W}$, $W_{\mu\nu}^i$ is the $SU(2)_L$ field strength, J^i is a generator of $SU(2)_L$, the sum over the index a is a sum over all pNGBs $\hat{\phi}$, and T^a is the generator of flavor $SU(N_f)$ corresponding to the a^{th} pNGB. It has been noticed that this operator vanishes for the $\hat{\pi}_3$ [11, 44, 73], and Refs. [11, 44] remarked that the G -even mesons can decay in this way, but the fact that the $\hat{\eta}_5$ is unique has not appeared in the literature. That is, if N_f is large enough such that an $\hat{\eta}_9, \hat{\eta}_{13}$, etc. exist in the spectrum, they do not have an anomaly with $SU(2)_L$, and so they do not decay like the $\hat{\eta}_5$. Recall from Sec. 2.1 that the $\hat{\eta}_5$ only exists in the spectrum if the quarks are in larger representations of $SU(2)_L$ than the fundamental, so studies with constituents in exclusively fundamental representations of their gauge groups would have missed this mechanism.

3.1 Review of Standard Model Meson Anomalies

First, we review the basics of the chiral anomalies that appear in QCD, which serve as an instructive comparison to the dark sector. They arise due to non-conservation of the chiral flavor currents j_μ^5 , such as the current corresponding to the axial $U(1)$ mentioned in Sec. 2.1. Consider the divergence of j_μ^{5a} due to SM gluons, with a indexing the generators that are broken during confinement:

$$\partial^\mu j_\mu^{5a} \propto G_{\text{SM}}^b \tilde{G}_{\text{SM}}^c \text{Tr} [T^a t^b t^c], \quad (3.2)$$

where G_{SM}^a is the QCD field strength, and t^a is a generator of $SU(3)_{\text{color}}$. The flavor generator T^a has flavor indices, while t^a has color indices, so the trace factorizes as

$$\text{Tr} [T^a t^b t^c] = \text{Tr} [T^a] \text{Tr} [t^b t^c] = 0, \quad (3.3)$$

since the flavor generator is traceless. However, if we consider the flavor-singlet η'_{SM} , the “flavor generator” is the identity in flavor space, which is not traceless, and the divergence becomes

$$\partial^\mu j_\mu^5 \propto G_{\text{SM}}^a \tilde{G}_{\text{SM}}^b \text{Tr} [t^a t^b] = \frac{1}{2} G_{\text{SM}}^a \tilde{G}_{\text{SM}}^a. \quad (3.4)$$

The flavor-singlet axial U(1) is therefore not a good symmetry of the UV theory, so the η'_{SM} is not a pNGB.

The SM pNGBs do not have an anomaly with QCD, but the neutral pion famously decays via an anomaly with QED. The effective operator governing this decay is

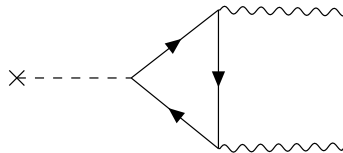
$$\mathcal{L}_{\text{anomaly}}^{\text{QED}} \propto \pi_{\text{SM}}^0 F \tilde{F} \text{Tr} [T^0 Q^2], \quad (3.5)$$

where F is the QED field strength, and the generators are

$$T^0 = \frac{1}{2} \begin{pmatrix} 1 & & \\ & -1 & \\ & & 0 \end{pmatrix}, \quad Q = \begin{pmatrix} 2/3 & & \\ & -1/3 & \\ & & -1/3 \end{pmatrix}, \quad (3.6)$$

which both have SU(3) flavor indices. The product $T^0 Q^2$ is not traceless, so this anomaly is non-vanishing.

We emphasize that the above anomalies are non-vanishing even though QED and QCD are vector-like theories. The flavor currents appearing in triangle diagrams of the form



are global chiral currents, so these global-gauge-gauge anomalies do not contradict the required absence of pure gauge anomalies. Each of these points is useful to keep in mind as we discuss the analogous anomalies in the dark sector.

3.2 Uniqueness of the 5-plet Anomaly

In this section, we study the anomalous interaction from Eq. (3.1) in detail. There is a simple argument from gauge invariance that the $\hat{\eta}_5$ is unique among the pNGBs in that it has an anomaly with $\text{SU}(2)_L$. We have an effective operator in Eq. (3.1) of the form $\hat{\pi} W \tilde{W}$ or $\hat{\eta} W \tilde{W}$. The W operators are in the $\mathbf{3}$ of $\text{SU}(2)_L$, and the $\hat{\pi}$ or $\hat{\eta}$ is in some representation \mathbf{d} . The effective operator can only be a gauge singlet if the product

$$\mathbf{3} \otimes \mathbf{3} \otimes \mathbf{d} = (\mathbf{1} \oplus \mathbf{3} \oplus \mathbf{5}) \otimes \mathbf{d} \quad (3.7)$$

contains a $\mathbf{1}$. This only occurs if \mathbf{d} is $\mathbf{1}$, $\mathbf{3}$, or $\mathbf{5}$, so only the $\hat{\eta}'$, $\hat{\pi}_3$, and $\hat{\eta}_5$ could have the anomaly. In light of the discussion in Sec. 3.1, it is unsurprising that the $\hat{\eta}'$ has an anomaly with $SU(2)_L$ in addition to $SU(N_c)$, but it is not a pNGB. This leaves only the $\hat{\pi}_3$ and $\hat{\eta}_5$, but the anomaly with the $\hat{\pi}_3$ vanishes for other reasons explained below.⁷

If the term in Eq. (3.1) with the $\hat{\pi}_3$ were non-vanishing, then it would clearly violate G -parity. However, we show here that this term vanishes regardless of G -violation in the UV (which further implies that the anomaly preserves G). Consider how one would determine the flavor generator T^a in Eq. (3.1) corresponding to a particular meson species in a particular multiplet. The flavor generator encodes the meson state as a linear combination of quark/anti-quark flavor states, which should be an eigenstate of the $SU(2)_L$ quadratic Casimir operator J^2 and the electric charge operator Q . Transformations of the meson state under $SU(2)_L$ can be written as transformations of T^a using

$$T^a \xrightarrow{J^i} [J^i, T^a], \quad (3.8)$$

where J^i is a generator of the N_f -dimensional representation of $SU(2)_L$. Then, the charge and Casimir operators act as

$$T^a \xrightarrow{Q} [J_z, T^a], \quad T^a \xrightarrow{J^2} [J^i, [J^i, T^a]]. \quad (3.9)$$

Therefore, the meson with charge Q in the $2J + 1$ -dimensional representation of $SU(2)_L$ corresponds to the flavor generator with

$$T^a \xrightarrow{Q} Q T^a, \quad T^a \xrightarrow{J^2} J(J + 1) T^a. \quad (3.10)$$

We provide a recipe to explicitly construct these generators in App. A. Suppose a meson's flavor generator is itself a linear combination of the $SU(2)_L$ generators. Then, its transformation under the Casimir operator is found using

$$J^a \xrightarrow{J^2} [J^i, [J^i, J^a]] = \varepsilon^{aij} \varepsilon^{ijk} J^k = 2J^a, \quad (3.11)$$

i.e. the meson is in the $J = 1$ (3-plet) representation. Thus, the flavor generators corresponding to the $\hat{\pi}_3$ multiplet are (unsurprisingly) linear combinations of $SU(2)_L$

⁷Outside of the context of our model, one could consider a minimal dark matter candidate that is the neutral component of a pseudoscalar $SU(2)_L$ 5-plet ϕ_5 . Using the UV-agnostic framework of Ref. [51], the $\phi_5 W \widetilde{W}$ effective operator (analogous to the anomaly operator in this work) would destabilize this dark matter candidate, and additional model building would be required for the UV completion to forbid this decay channel. This observation builds on the result of Ref. [51] that a *scalar* 5-plet minimal dark matter candidate can also be destabilized at dimension-5.

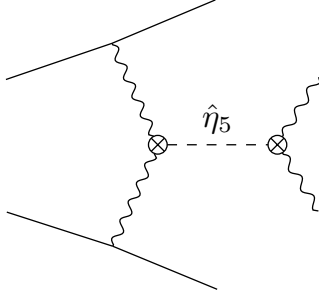


Figure 1: Feynman diagram corresponding to the anomaly-induced resonant production of the $\hat{\eta}_5$. The \otimes symbols denote insertions of the anomaly operator in Eq. (3.13). The $\hat{\eta}_5$ species are the unique pNGBs of dark chiral symmetry breaking with this operator. Observation of this signal provides sensitivity to UV parameters such as N_c and N_f , which set the strength of the coupling (see Eqs. (3.13) and (3.14)). LHC implications are discussed in Sec. 4.2.

generators. Then, the operator in Eq. (3.1) for the $\hat{\pi}_3$ contains

$$\varepsilon^{\mu\nu\alpha\beta} W_{\mu\nu}^i W_{\alpha\beta}^j \text{Tr} [J^a J^i J^j]. \quad (3.12)$$

Unlike the SM flavor and color generators in Eq. (3.3), the generators in this trace all have the same flavor indices (analogously to Eq. (3.5)), so the trace itself neither factorizes nor vanishes. However, the trace is anti-symmetric in the i and j indices,⁸ while $\varepsilon^{\mu\nu\alpha\beta} W_{\mu\nu}^i W_{\alpha\beta}^j$ is symmetric in i and j , so the operator vanishes. Therefore, the $\hat{\pi}_3$ does not have an anomaly with $\text{SU}(2)_L$. The flavor generators for meson multiplets besides the $\hat{\pi}_3$ are *not* linear combinations of $\text{SU}(2)_L$ generators, so the above argument does not forbid the $\hat{\eta}_5$ from having the anomaly.

In this way, we have shown that the $\hat{\eta}_5$ is the unique pNGB with a global- $\text{SU}(2)_L$ - $\text{SU}(2)_L$ anomaly. One can also see this by finding the generators for the $\hat{\pi}_7, \hat{\eta}_9$, *etc.* and observing that the trace in Eq. (3.1) for these species vanishes identically, unlike the trace in Eq. (3.12). Then, we can expand Eq. (3.1) as

$$\begin{aligned} \mathcal{L}_{\text{anomaly}} = c \frac{g_W^2}{16\pi^2} \frac{N_c}{f_\pi} \varepsilon^{\mu\nu\alpha\beta} & \left[\sqrt{\frac{3}{2}} \hat{\eta}_5^{++} (W_{\alpha\beta}^1 + iW_{\alpha\beta}^2)(W_{\mu\nu}^1 + iW_{\mu\nu}^2) \right. \\ & - \sqrt{6} \hat{\eta}_5^+ W_{\mu\nu}^3 (W_{\alpha\beta}^1 + iW_{\alpha\beta}^2) \\ & + \hat{\eta}_5^0 (2W_{\mu\nu}^3 W_{\alpha\beta}^3 - W_{\mu\nu}^1 W_{\alpha\beta}^1 - W_{\mu\nu}^2 W_{\alpha\beta}^2) \\ & + \sqrt{6} \hat{\eta}_5^- W_{\mu\nu}^3 (W_{\alpha\beta}^1 - iW_{\alpha\beta}^2) \\ & \left. + \sqrt{\frac{3}{2}} \hat{\eta}_5^{--} (W_{\alpha\beta}^1 - iW_{\alpha\beta}^2)(W_{\mu\nu}^1 - iW_{\mu\nu}^2) \right], \end{aligned} \quad (3.13)$$

⁸Equivalently, the totally symmetric invariant tensor d^{abc} of $\text{SU}(2)$ vanishes.

Species	SU(2) _L Rep.	$N_{f,\min}$	G -parity	Dominant decay
$\hat{\pi}_3$	3	2	-1	cascade ($\hat{\pi}_3^\pm$), G -violation ($\hat{\pi}_3^0$)
$\hat{\eta}_5$	5	3	+1	anomaly
$\hat{\pi}_7, \hat{\pi}_{11}, \hat{\pi}_{15}, \dots$	7, 11, 15, ...	4, 6, 8, ...	-1	hopping
$\hat{\eta}_9, \hat{\eta}_{13}, \hat{\eta}_{17}, \dots$	9, 13, 17, ...	5, 7, 9, ...	+1	

Table 1: Summary of the pNGBs of dark chiral symmetry breaking, including their representation under SU(2)_L, the minimum N_f such that the species exists in the spectrum (Sec. 2.1), the charge under the dark G -parity (Sec. 2.2), and the dominant decay mode (Secs. 2.2 and 3.2) for each meson. Decay modes specific to particular components of the SU(2)_L multiplets are specified. Several species decay via cascade, *i.e.* they decay to lighter meson in the same multiplet by radiating an off-shell gauge boson. The higher multiplets decay by hopping down to a lower multiplet with the same G -parity and emitting two gauge bosons.

where

$$c = \frac{1}{12\sqrt{10}} \sqrt{\frac{(N_f + 2)!}{(N_f - 3)!}} \quad (3.14)$$

is an overall coefficient derived in App. B. Since c scales as $N_f^{5/2}$, the strength of the anomaly interaction increases rather quickly with N_f . In the electroweak-broken phase, this operator leads to the decay of the $\hat{\eta}_5$ to different combinations of W^\pm , γ , and Z boson pairs.⁹ In addition, the anomaly also allows the $\hat{\eta}_5$ to be *resonantly produced* in proton-proton collisions via VBF [28],¹⁰ followed by decay to pairs of electroweak bosons, as shown in Fig. 1. The collider phenomenology of this global-gauge-gauge anomalous interaction is discussed in Sec. 4.2.

The anomaly is the dominant decay mode of each species in the 5-plet. One may have expected the singly-charged $\hat{\eta}^\pm$ mesons to decay analogously to the SM pion, *i.e.* via effectively mixing with the W boson. However, the operator $W_\mu^\pm \partial^\mu \pi_{\text{SM}}^\mp$ that leads to this mixing is parity-violating. The couplings of the W to the SM quarks violate parity, so this mixing operator naturally appears in the chiral Lagrangian. By contrast, the dark quarks have vector-like couplings to the W , so operators such as $W_\mu^\pm \partial^\mu \hat{\eta}^\mp$ are forbidden.

The anomaly allows one to probe some details of the UV theory while only measuring a few IR processes. The SU(N_f) generators T^a and SU(2)_L generators J^i in Eq. (3.1) depend on N_f , which causes the strength of the anomaly interaction also

⁹Since $W_{\mu\nu}^i$ is the full SU(2)_L non-abelian field strength, these operators also include couplings of the $\hat{\eta}_5$ to three electroweak bosons at higher order in g_W .

¹⁰See Ref. [74] for another example (in a composite Higgs context) of having a subset of mesons that can be produced through VBF via an anomaly.

Species	Production	Lifetime	Signal
$\hat{\pi}_3^\pm$	pairs via DY and VBF	$\mathcal{O}(0.1)$ ns	disappearing tracks
$\hat{\pi}_3^0$		collider-stable	
$\hat{\eta}_5^0, \hat{\eta}_5^\pm, \hat{\eta}_5^{\pm\pm}$	resonances via the anomaly	prompt	diboson decays

Table 2: Summary of the dark mesons we consider in our collider study.

to have dependence on N_f that is captured by the coefficient c in Eq. (3.14). In an idealized scenario, one could precisely measure the rate for some process involving self-interactions of the pNGBs to extract f_π , as well as the rates for the anomaly-induced processes to extract $c N_c/f_\pi$. Then, one may be able to reconstruct the UV parameters N_c and N_f . (Since N_c and N_f are discrete, the product $c N_c$ is usually not degenerate between different combinations of N_c and N_f .) This is analogous to using SM pion decay rates to extract the number of colors in QCD.

We have now explored each pNGB of chiral symmetry breaking and their decays, which are summarized in Table 1. In Sec. 4.2, we explore signals of resonant production of the $\hat{\eta}_5$. We only consider production and decay via the anomaly, which allows us to put an experimental bound on $4\pi f_\pi/N_c$ for a particular choice of N_f .

4 Collider Signals and Constraints

The results of Secs. 2 and 3 imply striking collider signals of the model’s dark mesons. A summary of the properties and signals of the pNGBs of dark chiral symmetry breaking is shown in Table 2. The $\hat{\pi}_3$ and $\hat{\eta}_5$ multiplets have entirely distinct and complementary signatures, each of which is the subject of several LHC searches. We use these searches to place constraints on the meson masses and the ratio f_π/N_c . For event generation, we use MADGRAPH5_AMC@NLO [75, 76] with a model we implement in FEYNRULES [77, 78]. For the LLP study, we use PYTHIA 8 [79] for showering and DELPHES 3 [80] with the default ATLAS card for detector simulation, which includes jet clustering using FASTJET [77, 78] with the anti- k_T clustering algorithm [81]. We generate events with zero, one, or two jets in the hard process, which are combined by MADGRAPH5 with matrix-level matching.

4.1 Disappearing Tracks: A 3-plet Signature

The $\hat{\pi}_3^\pm$ decays with a lifetime of $\mathcal{O}(0.1)$ ns to a neutral collider-stable $\hat{\pi}_3^0$ and a soft SM pion, which leads to the same kind of signal as the classic chargino decay to a neutralino in the Minimal Supersymmetric Standard Model when the wino is much lighter than all of the other superpartners. The charged particle leaves a few hits in the inner tracker before it decays, the soft SM pion is not reconstructed, and the

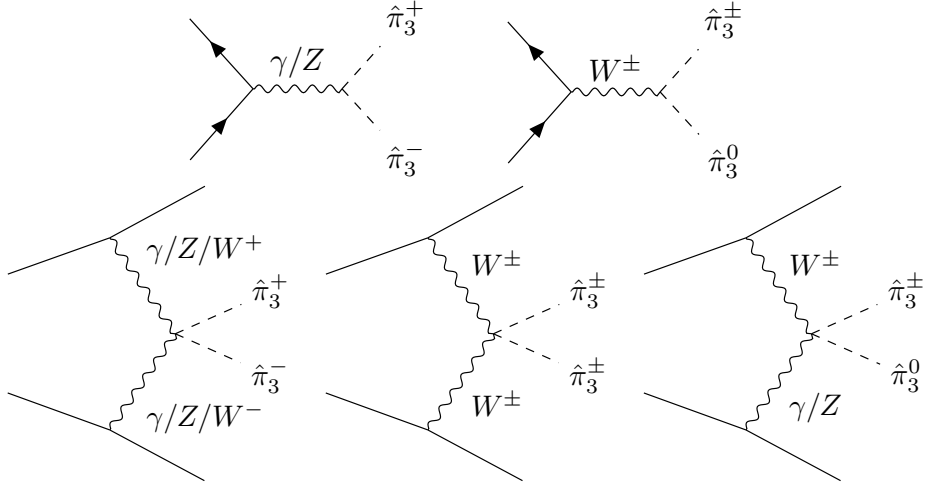


Figure 2: Diagrams representing pair production of the $\hat{\pi}_3$ mesons via Drell-Yan (top) and vector boson fusion (bottom). The VBF processes also get contributions from diagrams with three-point vertices coupling the mesons to vector bosons. Diagrams with production of two neutral mesons via VBF are not pictured, as we do not consider such processes.

result is a track that seems to stop inside the tracker.¹¹ These disappearing tracks signals are the subjects of recent searches by the ATLAS and CMS collaborations [83, 84], which place strong lower bounds on chargino masses.

The $\hat{\pi}_3$ is produced via DY and VBF in opposite charge, same charge, or charged-plus-neutral pairs, as pictured in Fig. 2. As has been pointed out in the contexts of sleptons and charginos [85, 86], the VBF cross section falls slower than that of DY as a function of mass, thus it can become the dominant process for masses above an $\mathcal{O}(100)$ GeV threshold. This effect is partially due to DY suffering from an s -channel propagator, while the vector bosons facilitating VBF can be light and close to on-shell. Another contribution to the enhancement of VBF over DY is that DY requires a sea anti-quark in the initial state, which has a suppressed parton distribution function compared to the quark initial states allowed in VBF. As shown in Fig. 3, we find that VBF dominates DY by a factor of $\mathcal{O}(100)$ for $m_\pi \gtrsim 700$ GeV in our case. This is a stronger enhancement than, for example, that of a selectron, in part due to the combinatorics involved in producing the various states within the $\hat{\pi}_3$ multiplet. The large production cross section allows us to place even stronger constraints on the $\hat{\pi}_3$ mass than existing constraints on chargino masses.

If $N_f \geq 4$, then there is a $\hat{\pi}_7$ in the meson spectrum in addition to the $\hat{\pi}_3$. The decays of the $\hat{\pi}_7$ to the $\hat{\pi}_3^\pm$ may also contribute to the disappearing tracks signal. However, these hopping decays (hopping from heavier to light pions with the same G -parity) are associated with additional SM states due to the emitted EW bosons,

¹¹There has been progress in reconstructing the soft SM pions that have $p_T \gtrsim 500$ MeV, which helps resolve the decay vertex and reject fake tracks that come from random hits [82].

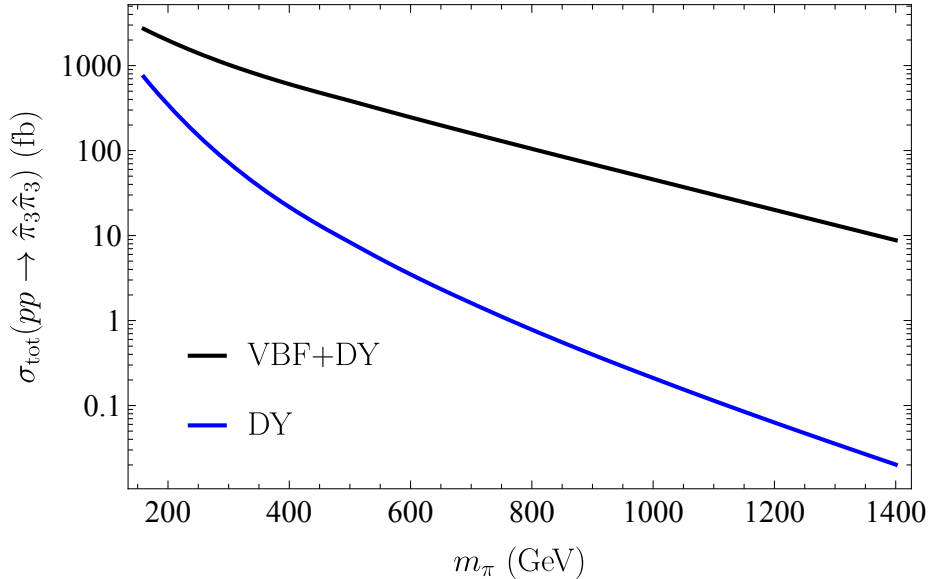


Figure 3: Total LHC production cross sections of the dark meson triplet $\hat{\pi}_3$ pairs we consider. The production rate for exclusively Drell-Yan processes falls much faster as a function of the $\hat{\pi}_3$ mass m_π than the rate of processes that include vector boson fusion.

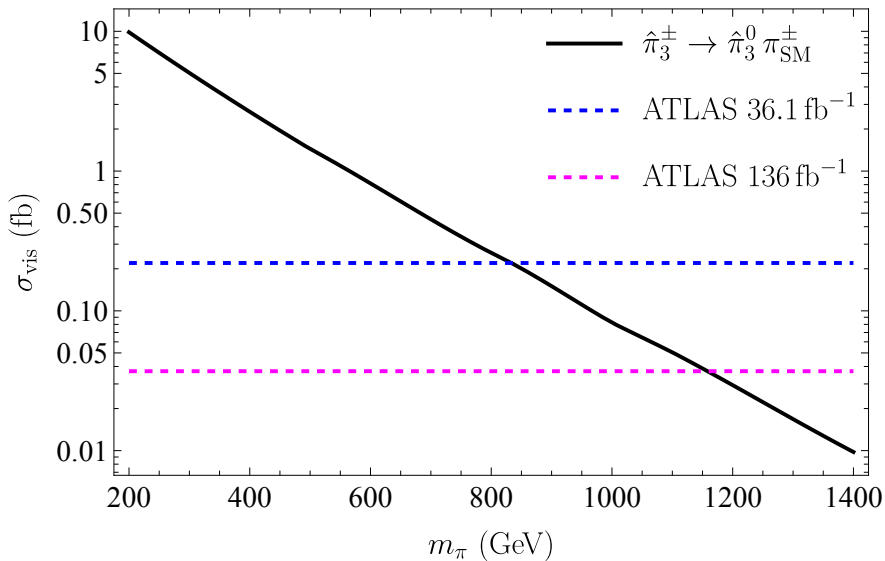


Figure 4: The visible cross section for production of disappearing tracks due to decays of the long-lived $\hat{\pi}_3^\pm$ meson. The dashed lines indicate model-independent upper bounds on this cross section based on the ATLAS searches in Refs. [83, 87] and using the re-interpretation methods provided by Ref. [64]. This shows a strong lower bound on the $\hat{\pi}_3$ meson mass m_π of ~ 1.2 TeV.

which complicates the disappearing tracks analysis. Therefore, we do not include the $\hat{\pi}_7$ (or larger multiplets present at higher N_f) in our analysis.

We re-use the methods from Ref. [64] available in the LLP Recasting Repository [88] to re-interpret two Run 2 ATLAS disappearing tracks searches.¹² The re-interpretation package enables us to compute the visible cross section, *i.e.* the product of the total production cross section and the efficiency of identifying a disappearing track. The first search, which the re-interpretation code was built for, used a dataset with an integrated luminosity of 36.1 fb^{-1} and placed a model-independent constraint on the visible cross section of disappearing tracks of 0.22 fb at the 95% confidence level [87]. The second search used an integrated luminosity of 136 fb^{-1} and found a constraint of 0.037 fb [83]. Our use of the more recent search limit on the visible cross section while taking advantage of the previous search re-interpretation methods provides a rough estimate that assumes the two searches have similar signal efficiencies. In Fig. 4 we show the visible cross section computed in our model as a function of the $\hat{\pi}_3$ mass. The efficiency is $\mathcal{O}(0.1)\%$ across the mass range in the figure. We find that the more recent search constrains the $\hat{\pi}_3$ mass to be $m_\pi \gtrsim 1.2 \text{ TeV}$.

The $\hat{\pi}_3$ production rate is independent of f_π , N_c , and N_f (unlike the resonance signature discussed in the upcoming section). This result therefore imposes a remarkably strong lower bound on the masses of all mesons in the spectrum, particularly since the $\hat{\pi}_3$ is the lightest state. Recall from Sec. 2.3 that the relationship between the $\hat{\pi}_3$ mass and the $\hat{\eta}_5$ mass m_η is somewhat uncertain due to its dependence on the UV cutoff of the meson EFT. Therefore, we cannot directly translate the bound on m_π into a bound on m_η , but we can estimate based on the scaling discussed in Sec. 2.3 that $m_\eta - m_\pi$ is roughly within an $\mathcal{O}(1)$ factor of f_π . This places an even larger lower bound on m_η that complements the constraints we show in Sec. 4.2.

4.2 Anomaly-induced Resonances: A 5-plet Signature

The $\hat{\eta}_5$ mesons can be singly produced through VBF and dominantly decay to pairs of electroweak bosons via the anomaly explained in Sec. 3.2 and shown in Fig. 1. Recall that while the $\hat{\pi}_3$ exists in the spectrum for all $N_f \geq 2$, the $\hat{\eta}_5$ is only present for $N_f \geq 3$. As a concrete benchmark, we set $N_f = 4$ in this section, but changing N_f simply modifies cross sections by $\mathcal{O}(1)$ factors explained in Eqs. (3.13) and (3.14). Setting $N_f = 4$ is a motivated choice, since it results in larger production rates than $N_f = 3$, and having $N_f \geq 5$ often leads to nearby Landau poles in the $SU(2)_L$ running coupling [50].

There are many LHC searches for resonances decaying to two electroweak bosons. Various final states have been exploited, including diphoton [94, 96], ZZ in the fully leptonic channel [90, 97], W^+W^- and/or ZZ in the semileptonic channel [91, 93], $W^\pm Z$ [89, 92], and same sign W pairs [92, 95]. Each of these searches quotes limits on the total production cross sections of a scalar resonantly produced via VBF and

¹²The most recent ATLAS and CMS searches in Refs. [83, 84] derived very similar model-dependent constraints on masses of supersymmetric particles, so we expect the CMS constraints on our model to be closely comparable.

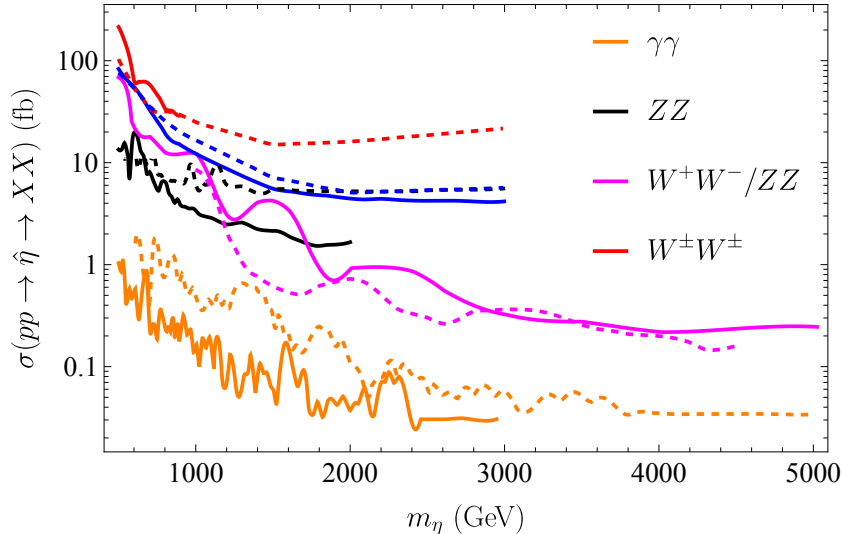


Figure 5: Upper bounds on the cross section to produce various final states from the searches in Refs. [89–97] through resonant production and decay of the scalar $\hat{\eta}$. Solid (dashed) lines correspond to ATLAS (CMS) searches. The ZZ searches used the fully leptonic channel, and the W^+W^-/ZZ searches used the semileptonic channel. In the context of our model, the $\hat{\eta}$ is one of the pNGBs of dark chiral symmetry breaking in the $SU(2)_L$ 5-plet. Besides the diphoton searches, each of these is specialized to production via VBF. We interpret these upper bounds as lower bounds on $4\pi f_\pi/N_c$ in Fig. 6.

decaying to each pair of bosons (except the diphoton searches, which do not specify the production channel).¹³

We show the upper limits on the cross sections from each search in Fig. 5.¹⁴ While the diphoton searches probe the lowest cross sections, the branching ratio of $\hat{\eta}_5^0 \rightarrow \gamma\gamma$ is about 4%, and the branching ratios to W^+W^- and ZZ are each roughly 1/3. Likewise, the same sign W searches tend to probe higher cross sections than other final states, but this is the principal decay mode of the $\hat{\eta}_5^{\pm\pm}$. Therefore, it is not obvious *a priori* which search imposes the strongest constraint on the model, and future searches for final states that currently impose weaker bounds may become competitive with searches for other final states if they attain greater signal efficiency.

To get a sense of the $\hat{\eta}_5$ decay widths, we can use the partial width

¹³The diphoton search in Ref. [94] quotes a limit on the fiducial cross section, which is defined in terms of generator-level cuts. These cuts modify our cross sections only by a small $\mathcal{O}(1)$ factor.

¹⁴The searches in Refs. [98, 99] target the γZ final state, which is a principal decay mode of the $\hat{\eta}_5^0$, but these specialize to the gluon-gluon fusion production channel, so we do not include them.

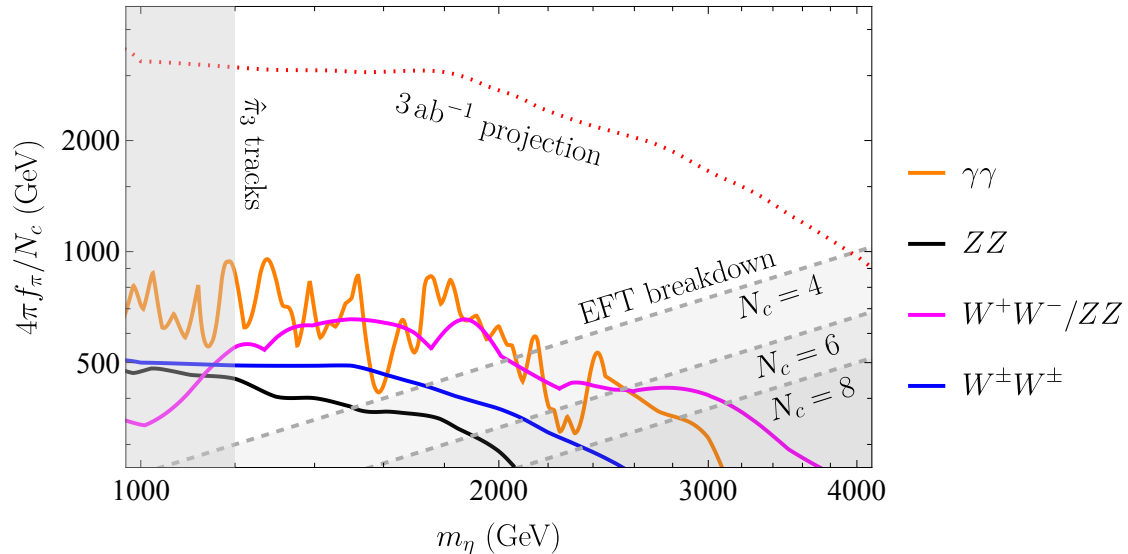


Figure 6: Lower bounds on the ratio $4\pi f_\pi/N_c$ as a function of the $\hat{\eta}_5$ meson mass m_η using the strongest constraints in Fig. 5 for each diboson final state. The gray contours indicate lower bounds on $4\pi f_\pi/N_c$ for a few values of N_c , below which $m_\eta > 4\pi f_\pi$ and the EFT of mesons breaks down. The region with $m_\eta < 1.2$ TeV is excluded by the disappearing tracks analysis in Sec. 4.1. The dotted red contour indicates a projection from a naïve luminosity rescaling of the expected limits of the searches with the strongest constraints on our model for a 3 ab^{-1} dataset.

$$\begin{aligned} \Gamma(\hat{\eta}_5^0 \rightarrow \gamma\gamma) &= \frac{2}{\pi} \alpha^2 m_\eta^3 \left(\frac{N_c}{4\pi f_\pi} \right)^2 \\ &\simeq 0.039 \text{ GeV} \left(\frac{m_\eta}{1 \text{ TeV}} \right)^3 \left(\frac{1 \text{ TeV}}{4\pi f_\pi/N_c} \right)^2, \end{aligned} \quad (4.1)$$

where $\alpha \simeq 1/128$ is the electromagnetic coupling, and $N_f = 4$. Since the branching ratio to diphoton is $\sim 4\%$, the total widths Γ_η are $\mathcal{O}(1)$ GeV when the other relevant mass scales are $\mathcal{O}(1)$ TeV. Likewise, the ratio Γ_η/m_η is $\mathcal{O}(10^{-3})$, so the narrow width approximation is valid in this regime.

In Fig. 6, we use the fact that the cross section scales as $(N_c/f_\pi)^2$ to recast the upper bounds on the production cross sections in Fig. 5 as lower bounds on the ratio $4\pi f_\pi/N_c$ as a function of m_η . The searches for diphoton and W^+W^-/ZZ in the semileptonic channel impose very similar constraints, and the same sign W and fully leptonic ZZ constraints are only an $\mathcal{O}(1)$ factor below. Constraints due to $W^\pm Z$ searches are not shown, as they are too weak to exclude any valid parameter space.

While we cannot precisely compute $m_\eta - m_\pi$, we know $m_\eta > m_\pi$, so the disappearing tracks analysis in Sec. 4.1 excludes the region where $m_\eta \lesssim 1.2$ TeV. The figure also shows contours where $m_\eta = 4\pi f_\pi$ for a few values of N_c . For values of f_π/N_c below these contours, one is probing the theory at a scale outside of the EFT's

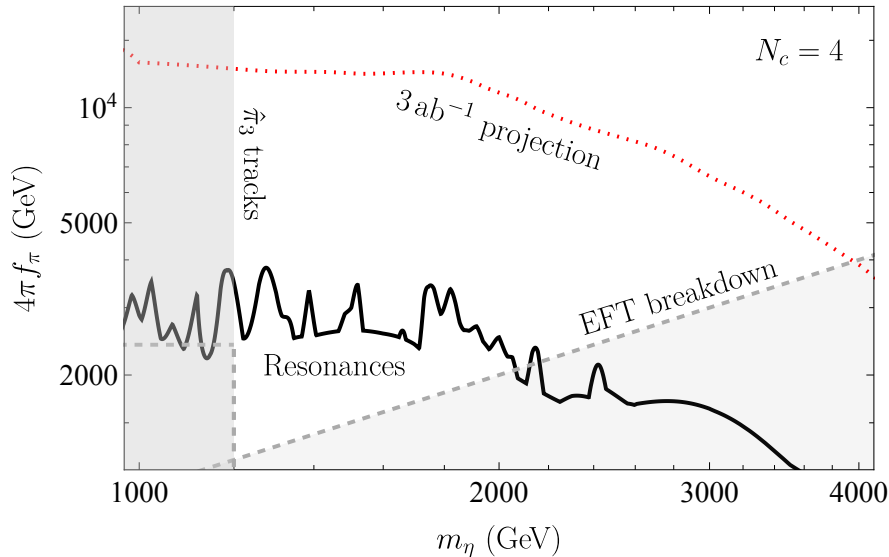


Figure 7: Lower bounds on $4\pi f_\pi$ as a function of the $\hat{\eta}_5$ meson mass m_η in the case of $N_c = 4$. Existing and projected resonance constraints due to the 5-plet anomaly, constraints from disappearing tracks due to the dark meson 3-plet $\hat{\pi}_3$, and the meson EFT breakdown where $m_\eta > 4\pi f_\pi$ are shown as in Fig. 6. The disappearing tracks constraint below $4\pi f_\pi = 2.4$ TeV is indicated by a dashed line, where pair production of $\hat{\pi}_3$ mesons with a mass of 1.2 TeV is outside the EFT regime of validity.

regime of validity, so that range of parameters is not physical. Our comparison of the $\hat{\pi}_3$ constraint with the $\hat{\eta}_5$ constraints presents another possible issue of EFT validity. The $\hat{\pi}_3$ pair production mechanisms we consider occur via marginal operators, so we can always implicitly enforce in Fig. 4 that the EFT scale $4\pi f_\pi$ is greater than the invariant mass of the $\hat{\pi}_3$ pairs. However, for smaller values of $4\pi f_\pi$ in Fig. 6, *pairs* of $\hat{\pi}_3$ mesons with masses of 1.2 TeV may have a greater invariant mass than the EFT scale, in which case the disappearing tracks constraint does not have a sensible interpretation within the EFT. This issue is most pronounced for smaller values of N_c .

In Fig. 7, we show the anomaly-induced resonance constraints for the choice of $N_c = 4$ and find that the bound on $4\pi f_\pi$ is greater than 2 TeV for the full $\hat{\eta}_5$ mass range within the EFT’s regime of validity. Recall from Sec. 2.3 that heavier meson resonances may become visible when $4\pi f_\pi \lesssim 2$ TeV. The figure shows that the anomaly-induced resonance signatures are at least competitive with those of the vector mesons, and they may be dominant. However, this 2 TeV estimate is predicated on a loose analogy between our model and the dark sector studied in Refs. [47] and [12]. The actual mass threshold where vector resonances gain importance depends strongly on details of the model such as N_c , the $\hat{\rho}/\hat{\pi}$ mass ratio, and the branching ratios of the $\hat{\rho}$ decays to other meson species. A thorough analysis of the vector meson phenomenology is beyond the scope of this work.

The constraints we derived in this section apply to meson mass scales up to multiple TeV and depend on f_π and N_c , while the disappearing tracks constraints in Sec. 4.1 apply to mass scales of ~ 1 TeV and do not depend (at least explicitly) on f_π or N_c . These two strategies are therefore complementary and represent exciting opportunities for future searches.

In Figs. 6 and 7, we also show projected bounds from a naïve luminosity rescaling of the expected limits from the searches with the strongest constraints on $4\pi f_\pi/N_c$. Specifically, we take the expected constraint on the cross section from each search, compute the corresponding constraints on $4\pi f_\pi/N_c$, and re-scale these constraints by $\sqrt{3 \text{ ab}^{-1}/L}$ with L each search’s luminosity. We then take the maximum of these re-scaled constraints for each value of m_η as the projected constraint. This projection demonstrates that if future searches attain similar signal efficiencies to existing searches, and if the High-Luminosity LHC acquires a dataset of 3 ab^{-1} , then such searches could reach a significantly larger region of parameter space.

5 Conclusion

This paper studied dark mesons arising in the confined phase of a strongly-coupled sector with vector-like dark quarks. We chose the dark quarks to be in the fundamental representation of a new confining $SU(N_c)$ and the N_f -dimensional representation of $SU(2)_L$. Considering the limit where the dark quark mass is much less than the dark confinement scale, we discussed the spectrum of $SU(2)_L$ representations of these mesons, their masses, and their transformations under various \mathbb{Z}_2 symmetries including a dark G -parity. We then studied two exotic collider signatures of the dark mesons in detail:

- The G -odd mesons are long-lived and therefore excellent targets for current and future LLP searches. In particular, the singly charged 3-plet $\hat{\pi}_3^\pm$ give rise to disappearing track signals.
- If $N_f \geq 3$, there is a G -even 5-plet meson $\hat{\eta}_5$ in the spectrum, which we showed is the unique pNGB of the dark sector chiral symmetry breaking that has an anomaly with $SU(2)_L$. This anomaly enables the $\hat{\eta}_5$ to be resonantly produced through VBF and decay to pairs of electroweak bosons with a rate that depends on N_c and the dark pion decay constant f_π .

We used the reinterpretation framework from Ref. [64] and the disappearing tracks searches in Refs. [87] and [83] to place a strikingly strong lower bound on the $\hat{\pi}_3$ mass m_π of ~ 1.2 TeV. We also used the searches for scalar resonances decaying to electroweak boson pairs in Refs. [90–97] to derive lower bounds on the ratio $4\pi f_\pi/N_c$ as a function of the $\hat{\eta}_5$ mass m_η . Measuring the rates of the anomaly-induced processes could help reconstruct N_c and N_f , thereby revealing a great deal about the

UV theory while only measuring states in the IR. These anomaly-induced resonances therefore remain an exciting target for diboson searches, including those using the unusual same sign W final state.

The model under study is an example of a confining dark sector with \mathcal{H} -parity [49]. The baryons in such models may be viable dark matter candidates that are characteristically challenging to probe via direct detection despite having constituents that are electrically charged. This is particularly true in the Noble Dark Matter case, where the dark matter candidate is either a total SM singlet or a singlet with a small mixing with other states [50]. As discussed in Refs. [49, 50], there are various opportunities for further analyzing the early universe dynamics, indirect detection, and astrophysical signatures of these dark matter scenarios. The results of this work show that a broad space of parameters with light 3-plet mesons or collider-scale 5-plet mesons is already ruled out, and future analyses can focus on other cases.

Several natural extensions of this work remain to be explored. While G -parity may stabilize some of the meson species on a detector timescale, the possibility of G violation by Planck-suppressed dimension-5 operators threatens the model's cosmological safety unless G is broken at a sub-Planckian scale that shortens the lifetime to below the timescale of Big Bang Nucleosynthesis. The lifetime could still be well beyond the detector scale, which is the case we consider in this work, but interesting new signals may emerge if the neutral $\hat{\pi}$ mesons can decay within the detector. For example, the $\hat{\pi}_3^\pm$ could leave a track that disappears within the tracker but points to a displaced energy deposit within the calorimeter where the $\hat{\pi}_3^0$ decays later. Measuring this process would probe the scale of G violation, and we leave the analysis of such signals for future work. Likewise, decays of pair-produced mesons in representations larger than the $\mathbf{5}$ that hop down to lower representations may lead to interesting signals from emission of multiple electroweak bosons, and measuring the rate for such processes would help reconstruct f_π .

We focused on the light quark limit with $4\pi f_\pi \gtrsim 2 \text{ TeV}$ because of the simplicity of the meson EFT. A smaller f_π would result in complications due to having a tower of lighter excited meson states. A natural direction for future studies would be to include consideration of the vector mesons in our model, along the lines of the discussion in Refs. [47] and [12] for a similar dark sector. Our dark $\hat{\rho}$ mesons can mix with the SM W and Z , leading to resonance signals that may be competitive with those discussed in this work when f_π is sufficiently small. The flavor-singlet $\hat{\eta}'$ may also play an important role as an additional anomaly-induced resonance.

Another small modification to our regime is the heavy quark limit (studied in Ref. [50] in the context of dark baryons). Here, producing dark sector states at a collider would probe the theory at a scale beyond the meson EFT's regime of validity. Instead, one would produce quirks [39], where a quark/anti-quark pair is joined by an unbroken flux tube and non-perturbatively radiates dark glueballs, photons, *etc.* before annihilating. Such a regime would have distinct signals from

those presented here that are also more difficult to model. An advantage of heavy quarks is the ability to compute the hadron mass spectrum in perturbation theory, thereby avoiding ambiguities such as the $\hat{\pi}_3$ - $\hat{\eta}_5$ mass splitting discussed above. One can also exploit the squeezeout mechanism in the heavy quark limit for determining the dark matter relic abundance of the dark baryons [100–102]. (In either the heavy- or light-quark limit, a matter/anti-matter asymmetry in the dark sector may be necessary for the dark baryons to have the relic abundance of dark matter [31, 100–102].) The light and heavy quark limits are therefore qualitatively different, and each merits further investigation.

The work presented here shows an example of how dark matter models with \mathcal{H} -parity can be (counter-intuitively) more easily discovered at colliders than other experiments searching for dark sectors with electroweak interactions. The 5-plet anomaly also serves as an example of how the rich spectra of confining dark sectors can enable a variety of counter-intuitive search strategies for physics beyond the Standard Model.

Acknowledgments

We thank Tom Bouley, Spencer Chang, Tim Cohen, Adam Martin, Nick Rodd for helpful discussions. The work of PA, AB, and GK is supported in part by the U.S. Department of Energy under grant number DE-SC0011640. EB is supported, in part, by the US National Science Foundation under Grant PHY-2210177. MC is supported in part by Perimeter Institute for Theoretical Physics. Research at Perimeter Institute is supported by the Government of Canada through the Department of Innovation, Science and Economic Development Canada and by the Province of Ontario through the Ministry of Research, Innovation and Science. SH is supported by the NSF grant PHY-2309456 and in part by the US-Israeli BSF grant 2016153. This research was supported in part by grant NSF PHY-2309135 to the Kavli Institute for Theoretical Physics (KITP). PA is grateful to the theory group at UC Santa Cruz for their kind hospitality and stimulating environment.

A Obtaining Flavor Generators

Here, we present a method to explicitly construct the flavor generators corresponding to meson species in specific $SU(2)_L$ multiplets with specific electric charges. One starts with a basis for the diagonal generators $\{D^a\}$ of $SU(N_f)$. For example,

$$D^1 = \frac{1}{2} \text{diag}(1, -1, 0, \dots, 0), \quad (\text{A.1})$$

$$D^2 = \frac{1}{2\sqrt{3}} \text{diag}(1, 1, -2, 0, \dots, 0), \quad (\text{A.2})$$

$$\dots, \quad (\text{A.3})$$

$$D^{N_f-1} = \frac{1}{\sqrt{2N_f(N_f-1)}} \text{diag}(1, \dots, 1, 1 - N_f). \quad (\text{A.4})$$

Then, one can define the matrix

$$M_{ab} = 2 \text{Tr} (D^a [J^i, [J^i, D^b]]), \quad (\text{A.5})$$

where J^i is a generator of the N_f -dimensional representation of $SU(2)_L$. As discussed in Sec. 3.2, the matrix M encodes the action of the quadratic Casimir operator of $SU(2)_L$ on the generators. The eigenvalues of M are $J(J+1)$ with $J \in \{1, 2, \dots, N_f - 1\}$, and the eigenvectors provide the linear combinations of the D^a generators corresponding to the neutral mesons in each of the $SU(2)_L$ representations $\mathbf{3}, \mathbf{5}, \dots, \mathbf{2N_f - 1}$. They must be the neutral mesons because the generators are diagonal and therefore commute with the third $SU(2)_L$ generator J_z . Now that one has the generators for the neutral mesons in each representation, one can construct the remaining flavor generators using the $SU(2)_L$ ladder operators

$$J^\pm = J_x \pm iJ_y, \quad (\text{A.6})$$

$$\langle m_1 | J^\pm | m_2 \rangle = \delta_{m_1, m_2 \pm 1} \sqrt{\frac{N_f^2 - 1}{4} - m_2(m_2 \pm 1)}, \quad (\text{A.7})$$

where J_x and J_y are the first and second $SU(2)_L$ generators. If T_J^Q is the flavor generator corresponding to the meson with charge Q in the $2J+1$ -dimensional representation of $SU(2)_L$, then one can raise or lower it to obtain

$$T_J^{Q\pm 1} = \frac{1}{\sqrt{J(J+1) - Q(Q \pm 1)}} [J^\pm, T_J^Q]. \quad (\text{A.8})$$

Each multiplet contains a neutral meson, so the iterative application of the ladder operators to the diagonal generators allows one to find the flavor generators for all meson species.

As an explicit example, consider the generators for the meson 5-plet $\hat{\eta}_5$ when $N_f = 3$. A basis for the diagonal generators of $SU(3)$ is

$$D^1 = \frac{1}{2} \begin{pmatrix} 1 & & \\ & -1 & \\ & & 0 \end{pmatrix}, \quad D^2 = \frac{1}{2\sqrt{3}} \begin{pmatrix} 1 & & \\ & 1 & \\ & & -1 \end{pmatrix}, \quad (\text{A.9})$$

with which one finds

$$M = \begin{pmatrix} 5 & -\sqrt{3} \\ -\sqrt{3} & 3 \end{pmatrix}. \quad (\text{A.10})$$

M has eigenvalues 2 and 6, as we expect from having 3-plet and 5-plet mesons. The eigenvectors of M show that the generator corresponding to the neutral 5-plet meson is

$$T_2^0 = \frac{\sqrt{3}}{2} D^1 - \frac{1}{2} D^2 = \frac{1}{2\sqrt{3}} \begin{pmatrix} 1 & & \\ & -2 & \\ & & 1 \end{pmatrix}. \quad (\text{A.11})$$

Then, using the ladder operators

$$J^+ = \sqrt{2} \begin{pmatrix} 0 & 1 & 0 \\ 0 & 0 & 1 \\ 0 & 0 & 0 \end{pmatrix}, \quad J^- = \sqrt{2} \begin{pmatrix} 0 & 0 & 0 \\ 1 & 0 & 0 \\ 0 & 1 & 0 \end{pmatrix} \quad (\text{A.12})$$

in combination with Eq. (A.8), one can construct the remaining 5-plet flavor generators

$$T_2^{++} = \frac{1}{\sqrt{2}} \begin{pmatrix} 0 & 0 & 1 \\ 0 & 0 & 0 \\ 0 & 0 & 0 \end{pmatrix}, \quad T_2^+ = \frac{1}{2} \begin{pmatrix} 0 & -1 & 0 \\ 0 & 0 & 1 \\ 0 & 0 & 0 \end{pmatrix}, \quad (\text{A.13})$$

$$T_2^{--} = \frac{1}{\sqrt{2}} \begin{pmatrix} 0 & 0 & 0 \\ 0 & 0 & 0 \\ 1 & 0 & 0 \end{pmatrix}, \quad T_2^- = \frac{1}{2} \begin{pmatrix} 0 & 0 & 0 \\ 1 & 0 & 0 \\ 0 & -1 & 0 \end{pmatrix}. \quad (\text{A.14})$$

This calculation helps establish the relative factors between different terms in the anomaly operator in Eq. (3.13), and the overall factor c is computed in App. B.

B Computing the 5-plet Anomaly

The coefficient c in Eq. (3.13) encodes the N_f dependence of the 5-plet anomaly. Here, we compute c for an arbitrary N_f using general properties of the 5-plet generators. To

start with a helpful analogy, recall from Sec. 3.2 that the generators corresponding to the 3-plet mesons are linear combinations of the $SU(2)_L$ generators J^i in the N_f -dimensional representation. This is expected, as J^i transforms as a **3**, so the generators of the **3** do so as well.

We can make a similar argument for the 5-plet by noticing that the **5** of $SU(2)$ is the symmetric traceless combination of two **3**'s. Therefore, the object

$$S^{ij} = \{J^i, J^j\} - \frac{1}{N_f} \text{Tr}(\{J^i, J^j\}) \mathbf{1}, \quad (\text{B.1})$$

where $\mathbf{1}$ is the identity in flavor space, is a tensor that transforms as a **5**. This means that the generators for the 5-plet mesons are linear combinations of the components of S^{ij} . To fully convince oneself of this, one can explicitly show

$$[J^k, [J^k, S^{ij}]] = 6S^{ij}, \quad (\text{B.2})$$

as required of the 5-plet generators (see Eq. (3.10)), using the identities

$$[J^k, [J^k, \{J^i, J^j\}]] = 6\{J^i, J^j\} - 4\delta^{ij}J^2 = 6\{J^i, J^j\} - (N_f^2 - 1)\delta^{ij} \mathbf{1}, \quad (\text{B.3})$$

and

$$\frac{1}{N_f} \text{Tr}(\{J^i, J^j\}) = \frac{1}{6}(N_f^2 - 1)\delta^{ij}. \quad (\text{B.4})$$

Then, the flavor generators corresponding to each 5-plet species are proportional to the components of S^{ij} in the spherical basis. In particular, the diagonal generator (corresponding to the neutral component of the 5-plet) is [103, 104]

$$\begin{aligned} T_2^0 &\propto \frac{1}{\sqrt{6}}(2S^{33} - S^{11} - S^{22}) \\ &\propto 3J_z^2 - J^2 = 3J_z^2 - \frac{N_f^2 - 1}{4} \mathbf{1}. \end{aligned} \quad (\text{B.5})$$

To enforce the normalization $\text{Tr}((T_2^0)^2) = 1/2$, we have

$$T_2^0 = \sqrt{10 \frac{(N_f - 3)!}{(N_f + 2)!}} \left(3J_z^2 - \frac{N_f^2 - 1}{4} \mathbf{1} \right), \quad (\text{B.6})$$

which follows from

$$J_z = \text{diag}((N_f - 1)/2, (N_f - 1)/2 - 1, \dots, -(N_f - 1)/2). \quad (\text{B.7})$$

The general form for T_2^0 will help us compute c .

The anomaly operator in Eq. (3.1) contains traces of the form

$$\text{Tr}(T^a J^i J^j). \quad (\text{B.8})$$

The a index picks out a particular meson species, and the i and j indices pick out particular components of the $\text{SU}(2)_L$ field strength $W_{\mu\nu}^i$. If we focus on the term with $i = j = 3$, we have

$$\mathcal{L}_{\text{anomaly}} \supset \frac{g_W^2}{16\pi^2} \frac{N_c}{f_\pi} \varepsilon^{\mu\nu\alpha\beta} W_{\mu\nu}^3 W_{\alpha\beta}^3 \hat{\eta}_5^0 \text{Tr}(T_2^0 J_z^2). \quad (\text{B.9})$$

The relative factors between the traces over different combinations of generators are fixed by gauge invariance, so it is sufficient to compute only one of them for an arbitrary N_f , and c is an overall factor in the anomaly operator. Thus, we can match Eq. (B.9) onto Eq. (3.13) to conclude

$$\begin{aligned} c &= \frac{1}{2} \text{Tr}(T_2^0 J_z^2) \\ &= \frac{1}{12\sqrt{10}} \sqrt{\frac{(N_f + 2)!}{(N_f - 3)!}}. \end{aligned} \quad (\text{B.10})$$

This tells us how the strength of the anomaly interaction varies with N_f .

References

- [1] CMS collaboration, *Search for resonant production of strongly coupled dark matter in proton-proton collisions at 13 TeV*, *JHEP* **06** (2022) 156 [[2112.11125](#)].
- [2] ATLAS collaboration, *Search for non-resonant production of semi-visible jets using Run 2 data in ATLAS*, *Phys. Lett. B* **848** (2024) 138324 [[2305.18037](#)].
- [3] CMS collaboration, *Search for dark QCD with emerging jets in proton-proton collisions at $\sqrt{s} = 13$ TeV*, *JHEP* **07** (2024) 142 [[2403.01556](#)].
- [4] ATLAS collaboration, *Search for dark mesons decaying to top and bottom quarks in proton-proton collisions at $\sqrt{s} = 13$ TeV with the ATLAS detector*, *JHEP* **09** (2024) 005 [[2405.20061](#)].
- [5] CMS collaboration, *Search for Soft Unclustered Energy Patterns in Proton-Proton Collisions at 13 TeV*, *Phys. Rev. Lett.* **133** (2024) 191902 [[2403.05311](#)].
- [6] CMS collaboration, *Search for soft unclustered energy patterns in association with a Z boson in proton-proton collisions at 13 TeV*, Tech. Rep. [CMS-PAS-EXO-23-003](#) (2025).
- [7] CMS collaboration, *Search for low-mass hidden valley dark showers with displaced dimuons in proton-proton collisions at $\sqrt{s} = 13$ TeV*, Tech. Rep. [CMS-PAS-EXO-24-008](#) (2025).

- [8] CMS collaboration, *Search for soft unclustered energy patterns in association with a W boson in proton-proton collisions at 13 TeV*, Tech. Rep. [CMS-PAS-EXO-24-030](#) (2025).
- [9] ATLAS collaboration, *Search for new physics in final states with semi-visible jets or anomalous signatures using the ATLAS detector*, [2505.01634](#).
- [10] ATLAS collaboration, *Search for emerging jets in pp collisions at $\sqrt{s} = 13.6$ TeV with the ATLAS experiment*, [2505.02429](#).
- [11] D. Barducci, S. De Curtis, M. Redi and A. Tesi, *An almost elementary Higgs: Theory and Practice*, *JHEP* **08** (2018) 017 [[1805.12578](#)].
- [12] G.D. Kribs, A. Martin, B. Ostdiek and T. Tong, *Dark Mesons at the LHC*, *JHEP* **07** (2019) 133 [[1809.10184](#)].
- [13] R. Contino, A. Podo and F. Revello, *Composite Dark Matter from Strongly-Interacting Chiral Dynamics*, *JHEP* **02** (2021) 091 [[2008.10607](#)].
- [14] H. Mies, C. Scherb and P. Schwaller, *Collider constraints on dark mediators*, *JHEP* **04** (2021) 049 [[2011.13990](#)].
- [15] J.M. Butterworth, L. Corpe, X. Kong, S. Kulkarni and M. Thomas, *New sensitivity of LHC measurements to composite dark matter models*, *Phys. Rev. D* **105** (2022) 015008 [[2105.08494](#)].
- [16] C. Kilic, T. Okui and R. Sundrum, *Vectorlike Confinement at the LHC*, *JHEP* **02** (2010) 018 [[0906.0577](#)].
- [17] C. Kilic and T. Okui, *The LHC Phenomenology of Vectorlike Confinement*, *JHEP* **04** (2010) 128 [[1001.4526](#)].
- [18] R. Harnik, G.D. Kribs and A. Martin, *Quirks at the Tevatron and Beyond*, *Phys. Rev. D* **84** (2011) 035029 [[1106.2569](#)].
- [19] P. Schwaller, D. Stolarski and A. Weiler, *Emerging Jets*, *JHEP* **05** (2015) 059 [[1502.05409](#)].
- [20] R. Mahbubani, P. Schwaller and J. Zurita, *Closing the window for compressed Dark Sectors with disappearing charged tracks*, *JHEP* **06** (2017) 119 [[1703.05327](#)].
- [21] O. Buchmueller, A. De Roeck, K. Hahn, M. McCullough, P. Schwaller, K. Sung et al., *Simplified Models for Displaced Dark Matter Signatures*, *JHEP* **09** (2017) 076 [[1704.06515](#)].
- [22] S. Renner and P. Schwaller, *A flavoured dark sector*, *JHEP* **08** (2018) 052 [[1803.08080](#)].
- [23] H.-C. Cheng, L. Li, E. Salvioni and C.B. Verhaaren, *Light Hidden Mesons through the Z Portal*, *JHEP* **11** (2019) 031 [[1906.02198](#)].
- [24] A. Batz, T. Cohen, D. Curtin, C. Gemmeil and G.D. Kribs, *Dark sector glueballs at the LHC*, *JHEP* **04** (2024) 070 [[2310.13731](#)].

- [25] M.J. Strassler and K.M. Zurek, *Echoes of a hidden valley at hadron colliders*, *Phys. Lett. B* **651** (2007) 374 [[hep-ph/0604261](#)].
- [26] T. Han, Z. Si, K.M. Zurek and M.J. Strassler, *Phenomenology of hidden valleys at hadron colliders*, *JHEP* **07** (2008) 008 [[0712.2041](#)].
- [27] T. Cohen, M. Lisanti and H.K. Lou, *Semivisible Jets: Dark Matter Undercover at the LHC*, *Phys. Rev. Lett.* **115** (2015) 171804 [[1503.00009](#)].
- [28] O. Antipin, M. Redi, A. Strumia and E. Vigiani, *Accidental Composite Dark Matter*, *JHEP* **07** (2015) 039 [[1503.08749](#)].
- [29] S. Knapen, S. Pagan Griso, M. Papucci and D.J. Robinson, *Triggering Soft Bombs at the LHC*, *JHEP* **08** (2017) 076 [[1612.00850](#)].
- [30] T. Cohen, M. Lisanti, H.K. Lou and S. Mishra-Sharma, *LHC Searches for Dark Sector Showers*, *JHEP* **11** (2017) 196 [[1707.05326](#)].
- [31] A. Mitridate, M. Redi, J. Smirnov and A. Strumia, *Dark Matter as a weakly coupled Dark Baryon*, *JHEP* **10** (2017) 210 [[1707.05380](#)].
- [32] A. Pierce, B. Shakya, Y. Tsai and Y. Zhao, *Searching for confining hidden valleys at LHCb, ATLAS, and CMS*, *Phys. Rev. D* **97** (2018) 095033 [[1708.05389](#)].
- [33] H. Beauchesne, E. Bertuzzo, G. Grilli Di Cortona and Z. Tabrizi, *Collider phenomenology of Hidden Valley mediators of spin 0 or 1/2 with semivisible jets*, *JHEP* **08** (2018) 030 [[1712.07160](#)].
- [34] E. Bernreuther, T. Finke, F. Kahlhoefer, M. Krämer and A. Mück, *Casting a graph net to catch dark showers*, *SciPost Phys.* **10** (2021) 046 [[2006.08639](#)].
- [35] S. Knapen, J. Shelton and D. Xu, *Perturbative benchmark models for a dark shower search program*, *Phys. Rev. D* **103** (2021) 115013 [[2103.01238](#)].
- [36] J. Barron, D. Curtin, G. Kasieczka, T. Plehn and A. Spourdalakis, *Unsupervised hadronic SUEP at the LHC*, *JHEP* **12** (2021) 129 [[2107.12379](#)].
- [37] H.-C. Cheng, L. Li and E. Salvioni, *A theory of dark pions*, *JHEP* **01** (2022) 122 [[2110.10691](#)].
- [38] S. Born, R. Karur, S. Knapen and J. Shelton, *Scouting for dark showers at CMS and LHCb*, *Phys. Rev. D* **108** (2023) 035034 [[2303.04167](#)].
- [39] J. Kang and M.A. Luty, *Macroscopic Strings and 'Quirks' at Colliders*, *JHEP* **11** (2009) 065 [[0805.4642](#)].
- [40] S. Knapen, H.K. Lou, M. Papucci and J. Setford, *Tracking down Quirks at the Large Hadron Collider*, *Phys. Rev. D* **96** (2017) 115015 [[1708.02243](#)].
- [41] J.A. Evans and M.A. Luty, *Stopping Quirks at the LHC*, *JHEP* **06** (2019) 090 [[1811.08903](#)].
- [42] G.D. Kribs and E.T. Neil, *Review of strongly-coupled composite dark matter models and lattice simulations*, *Int. J. Mod. Phys. A* **31** (2016) 1643004 [[1604.04627](#)].

- [43] G. Albouy et al., *Theory, phenomenology, and experimental avenues for dark showers: a Snowmass 2021 report*, *Eur. Phys. J. C* **82** (2022) 1132 [2203.09503].
- [44] Y. Bai and R.J. Hill, *Weakly Interacting Stable Pions*, *Phys. Rev. D* **82** (2010) 111701 [1005.0008].
- [45] O. Antipin, M. Redi and A. Strumia, *Dynamical generation of the weak and Dark Matter scales from strong interactions*, *JHEP* **01** (2015) 157 [1410.1817].
- [46] T. Appelquist et al., *Stealth Dark Matter: Dark scalar baryons through the Higgs portal*, *Phys. Rev. D* **92** (2015) 075030 [1503.04203].
- [47] G.D. Kribs, A. Martin and T. Tong, *Effective Theories of Dark Mesons with Custodial Symmetry*, *JHEP* **08** (2019) 020 [1809.10183].
- [48] T. Abe, R. Sato and T. Yamanaka, *Composite Dark Matter with Forbidden Annihilation*, 2404.03963.
- [49] P. Asadi, G.D. Kribs and C.J.H. Mantel, *Direct detection of dark baryons naturally suppressed by \mathcal{H} -parity*, *Phys. Rev. D* **111** (2025) 095030 [2410.23631].
- [50] P. Asadi, A. Batz and G.D. Kribs, *Noble dark matter: Surprising elusiveness of dark baryons*, *Phys. Rev. D* **111** (2025) 095025 [2412.14240].
- [51] M. Cirelli, N. Fornengo and A. Strumia, *Minimal dark matter*, *Nucl. Phys. B* **753** (2006) 178 [hep-ph/0512090].
- [52] A.J. Barr, C.G. Lester, M.A. Parker, B.C. Allanach and P. Richardson, *Discovering anomaly mediated supersymmetry at the LHC*, *JHEP* **03** (2003) 045 [hep-ph/0208214].
- [53] N.E. Bomark, A. Kvellestad, S. Lola, P. Osland and A.R. Raklev, *Long lived charginos in Natural SUSY?*, *JHEP* **05** (2014) 007 [1310.2788].
- [54] Y. Nakai, R. Sato and K. Tobioka, *Footprints of New Strong Dynamics via Anomaly and the 750 GeV Diphoton*, *Phys. Rev. Lett.* **116** (2016) 151802 [1512.04924].
- [55] Y. Bai, J. Berger and R. Lu, *750 GeV dark pion: Cousin of a dark G -parity odd WIMP*, *Phys. Rev. D* **93** (2016) 076009 [1512.05779].
- [56] G. Elor, H. Liu, T.R. Slatyer and Y. Soreq, *Complementarity for Dark Sector Bound States*, *Phys. Rev. D* **98** (2018) 036015 [1801.07723].
- [57] S. Bottaro, A. Strumia and N. Vignaroli, *Minimal Dark Matter bound states at future colliders*, *JHEP* **06** (2021) 143 [2103.12766].
- [58] T.D. Lee and C.N. Yang, *Charge conjugation, a new quantum number g , and selection rules concerning a nucleon-antinucleon system*, *Il Nuovo Cimento (1955-1965)* **3** (1956) 749.
- [59] PARTICLE DATA GROUP collaboration, *Review of particle physics*, *Phys. Rev. D* **110** (2024) 030001.
- [60] B.M.K. Nefkens and J.W. Price, *The Neutral decay modes of the eta meson*, *Phys. Scripta T* **99** (2002) 114 [nucl-ex/0202008].

- [61] K. Jedamzik, *Big bang nucleosynthesis constraints on hadronically and electromagnetically decaying relic neutral particles*, *Phys. Rev. D* **74** (2006) 103509 [[hep-ph/0604251](#)].
- [62] M. Kawasaki, K. Kohri, T. Moroi, K. Murai and H. Murayama, *Big-bang nucleosynthesis with sub-GeV massive decaying particles*, *JCAP* **12** (2020) 048 [[2006.14803](#)].
- [63] A. Belyaev, G. Cacciapaglia, I.P. Ivanov, F. Rojas-Abatte and M. Thomas, *Anatomy of the Inert Two Higgs Doublet Model in the light of the LHC and non-LHC Dark Matter Searches*, *Phys. Rev. D* **97** (2018) 035011 [[1612.00511](#)].
- [64] A. Belyaev, S. Prestel, F. Rojas-Abbate and J. Zurita, *Probing dark matter with disappearing tracks at the LHC*, *Phys. Rev. D* **103** (2021) 095006 [[2008.08581](#)].
- [65] E. Witten, *Large n chiral dynamics*, *Annals of Physics* **128** (1980) 363.
- [66] ATLAS collaboration, *Search for new high-mass phenomena in the dilepton final state using 36 fb^{-1} of proton-proton collision data at $\sqrt{s} = 13 \text{ TeV}$ with the ATLAS detector*, *JHEP* **10** (2017) 182 [[1707.02424](#)].
- [67] CMS collaboration, *Search for high-mass resonances in dilepton final states in proton-proton collisions at $\sqrt{s} = 13 \text{ TeV}$* , *JHEP* **06** (2018) 120 [[1803.06292](#)].
- [68] J. Wess and B. Zumino, *Consequences of anomalous Ward identities*, *Phys. Lett. B* **37** (1971) 95.
- [69] E. Witten, *Global Aspects of Current Algebra*, *Nucl. Phys. B* **223** (1983) 422.
- [70] E. Witten, *Nonabelian Bosonization in Two-Dimensions*, *Commun. Math. Phys.* **92** (1984) 455.
- [71] M.E. Peskin and D.V. Schroeder, *An Introduction to quantum field theory*, Addison-Wesley, Reading, USA (1995).
- [72] D. Tong, “Gauge theory.” <https://www.damtp.cam.ac.uk/user/tong/gaugetheory.html>, 2018.
- [73] K. Howe, S. Knapen and D.J. Robinson, *Diphotons from electroweak triplet-singlet mixing*, *Phys. Rev. D* **94** (2016) 035021 [[1603.08932](#)].
- [74] M.J. Dugan, H. Georgi and D.B. Kaplan, *Anatomy of a Composite Higgs Model*, *Nucl. Phys. B* **254** (1985) 299.
- [75] J. Alwall, R. Frederix, S. Frixione, V. Hirschi, F. Maltoni, O. Mattelaer et al., *The automated computation of tree-level and next-to-leading order differential cross sections, and their matching to parton shower simulations*, *JHEP* **07** (2014) 079 [[1405.0301](#)].
- [76] R. Frederix, S. Frixione, V. Hirschi, D. Pagani, H.S. Shao and M. Zaro, *The automation of next-to-leading order electroweak calculations*, *JHEP* **07** (2018) 185 [[1804.10017](#)].

- [77] M. Cacciari and G.P. Salam, *Dispelling the N^3 myth for the k_t jet-finder*, *Phys. Lett. B* **641** (2006) 57 [[hep-ph/0512210](#)].
- [78] M. Cacciari, G.P. Salam and G. Soyez, *FastJet User Manual*, *Eur. Phys. J. C* **72** (2012) 1896 [[1111.6097](#)].
- [79] C. Bierlich et al., *A comprehensive guide to the physics and usage of PYTHIA 8.3*, *SciPost Phys. Codeb.* **2022** (2022) 8 [[2203.11601](#)].
- [80] DELPHES 3 collaboration, *DELPHES 3, A modular framework for fast simulation of a generic collider experiment*, *JHEP* **02** (2014) 057 [[1307.6346](#)].
- [81] M. Cacciari, G.P. Salam and G. Soyez, *The anti- k_t jet clustering algorithm*, *JHEP* **04** (2008) 063 [[0802.1189](#)].
- [82] ATLAS collaboration, *Performance of tracking and vertexing techniques for a disappearing track plus soft track signature with the ATLAS detector*, Tech. Rep. [ATL-PHYS-PUB-2019-011](#) (2019).
- [83] ATLAS collaboration, *Search for long-lived charginos based on a disappearing-track signature using 136 fb^{-1} of pp collisions at $\sqrt{s} = 13 \text{ TeV}$ with the ATLAS detector*, *Eur. Phys. J. C* **82** (2022) 606 [[2201.02472](#)].
- [84] CMS collaboration, *Search for supersymmetry in final states with disappearing tracks in proton-proton collisions at $s=13 \text{ TeV}$* , *Phys. Rev. D* **109** (2024) 072007 [[2309.16823](#)].
- [85] A. Datta, P. Konar and B. Mukhopadhyaya, *Invisible charginos and neutralinos from gauge boson fusion: A Way to explore anomaly mediation?*, *Phys. Rev. Lett.* **88** (2002) 181802 [[hep-ph/0111012](#)].
- [86] D. Choudhury, A. Datta, K. Huitu, P. Konar, S. Moretti and B. Mukhopadhyaya, *Slepton production from gauge boson fusion*, *Phys. Rev. D* **68** (2003) 075007 [[hep-ph/0304192](#)].
- [87] ATLAS collaboration, *Search for long-lived charginos based on a disappearing-track signature in pp collisions at $\sqrt{s} = 13 \text{ TeV}$ with the ATLAS detector*, *JHEP* **06** (2018) 022 [[1712.02118](#)].
- [88] G. Cottin, N. Desai, S. Kraml and A. Lessa, “LLP Recasting Repository.” <https://github.com/llprecasting/recastingCodes/>, 2019.
- [89] ATLAS collaboration, *Search for resonant WZ production in the fully leptonic final state in proton-proton collisions at $\sqrt{s} = 13 \text{ TeV}$ with the ATLAS detector*, *Phys. Lett. B* **787** (2018) 68 [[1806.01532](#)].
- [90] ATLAS collaboration, *Search for heavy resonances decaying into a pair of Z bosons in the $\ell^+\ell^-\ell'^+\ell'^-$ and $\ell^+\ell^-\nu\bar{\nu}$ final states using 139 fb^{-1} of proton-proton collisions at $\sqrt{s} = 13 \text{ TeV}$ with the ATLAS detector*, *Eur. Phys. J. C* **81** (2021) 332 [[2009.14791](#)].
- [91] ATLAS collaboration, *Search for heavy diboson resonances in semileptonic final*

- states in pp collisions at $\sqrt{s} = 13$ TeV with the ATLAS detector, *Eur. Phys. J. C* **80** (2020) 1165 [[2004.14636](#)].
- [92] CMS collaboration, *Search for charged Higgs bosons produced in vector boson fusion processes and decaying into vector boson pairs in proton–proton collisions at $\sqrt{s} = 13$ TeV*, *Eur. Phys. J. C* **81** (2021) 723 [[2104.04762](#)].
- [93] CMS collaboration, *Search for heavy resonances decaying to WW , WZ , or WH boson pairs in the lepton plus merged jet final state in proton–proton collisions at $\sqrt{s} = 13$ TeV*, *Phys. Rev. D* **105** (2022) 032008 [[2109.06055](#)].
- [94] ATLAS collaboration, *Search for resonances decaying into photon pairs in 139 fb^{-1} of pp collisions at $\sqrt{s}=13$ TeV with the ATLAS detector*, *Phys. Lett. B* **822** (2021) 136651 [[2102.13405](#)].
- [95] ATLAS collaboration, *Measurement and interpretation of same-sign W boson pair production in association with two jets in pp collisions at $\sqrt{s} = 13$ TeV with the ATLAS detector*, *JHEP* **04** (2024) 026 [[2312.00420](#)].
- [96] CMS collaboration, *Search for new physics in high-mass diphoton events from proton–proton collisions at $\sqrt{s} = 13$ TeV*, *JHEP* **08** (2024) 215 [[2405.09320](#)].
- [97] CMS collaboration, *Search for heavy scalar resonances decaying to a pair of Z bosons in the 4-lepton final state at 13 TeV*, Tech. Rep. [CMS-PAS-HIG-24-002](#) (2024).
- [98] ATLAS collaboration, *Search for heavy resonances decaying to a Z boson and a photon in pp collisions at $\sqrt{s} = 13$ TeV with the ATLAS detector*, *Phys. Lett. B* **764** (2017) 11 [[1607.06363](#)].
- [99] CMS collaboration, *Search for high-mass $Z\gamma$ resonances in $e^+e^-\gamma$ and $\mu^+\mu^-\gamma$ final states in proton–proton collisions at $\sqrt{s} = 8$ and 13 TeV*, *JHEP* **01** (2017) 076 [[1610.02960](#)].
- [100] P. Asadi, E.D. Kramer, E. Kuflik, G.W. Ridgway, T.R. Slatyer and J. Smirnov, *Thermal squeezeout of dark matter*, *Phys. Rev. D* **104** (2021) 095013 [[2103.09827](#)].
- [101] P. Asadi, E.D. Kramer, E. Kuflik, G.W. Ridgway, T.R. Slatyer and J. Smirnov, *Accidentally Asymmetric Dark Matter*, *Phys. Rev. Lett.* **127** (2021) 211101 [[2103.09822](#)].
- [102] P. Asadi, E.D. Kramer, E. Kuflik, T.R. Slatyer and J. Smirnov, *Glueballs in a thermal squeezeout model*, *JHEP* **07** (2022) 006 [[2203.15813](#)].
- [103] D.A. Varshalovich, A.N. Moskalev and V.K. Khersonskii, *Quantum Theory of Angular Momentum: Irreducible Tensors, Spherical Harmonics, Vector Coupling Coefficients, 3nj Symbols*, World Scientific Publishing Company (1988), [10.1142/0270](#).
- [104] J.J. Sakurai and J. Napolitano, *Modern Quantum Mechanics*, Quantum physics, quantum information and quantum computation, Cambridge University Press, 3 ed. (10, 2020), [10.1017/9781108587280](#).